Computer Simulation of Stand-alone Photovoltaic Systems with Battery Storage

Philip Clifford Geerdts

Cape Town

December 1991

Submitted to the University of Cape Town in partial fulfillment of the requirements for the degree of Master of Science in Engineering.

DECLARATION

I declare that this dissertation is my own original work. It is being submitted in partial fulfillment for the degree of Master of Science in Engineering at the University of Cape Town. It has not been submitted before for any degree or examination at any university.

Signed by candidate

P C Geerdts

28th day of December 1991

ACKNOWLEDGEMENTS

It gives me great pleasure to acknowledge the contribution that the following people have made to this project:

- the National Energy Council for their financial backing,
- Anton Eberhard for his challenging supervision and resourceful guidance,
- Bill Cowan for his supervision and assistance towards the final stages of the project,
- Christopher Purcell for his perceptive ideas, and
- my parents and friends for their consistent support.

SYNOPSIS

This report describes a computer program which has been developed to simulate accurately the performance of stand alone photovoltaic systems with battery storage on an hourly basis for one simulated year.

The program incorporates models of the POA irradiance, the photovoltaic cell temperature and the battery temperature to simulate the environmental conditions of the system. These require hourly weather data as input. Typical meteorological years, which constitute a suitable form of input weather data, have been generated for those weather stations in Southern Africa which contain sufficient data.

The energy flows within the system are simulated using models of the following parameters: photovoltaic module current, regulator efficiency and voltage, battery current and voltage, inverter efficiency, load shed voltage and load current. These models incorporate versatility in the level of modelling complexity (determined typically by the availability of the data used to characterise the components).

The various models are encapsulated in modular units to facilitate alteration and updating at a later stage.

The program is designed to simulate photovoltaic systems without maximum power point trackers, necessitating the use of interactive curve solving to compute the system operating point at any time. A robust and comprehensive algorithm has been implemented to execute this function.

Improved battery modelling has been effected using data and experience acquired from a parallel research project.

The program facilitates, with the judicious selection of input weather data, the economical sizing of systems in that it incorporates loss of power probability analysis and offers a high level of modelling precision.

The simulation performance of the program compared favourably with that of PVFORM. The system performance estimated by PVFORM was marginally better, which is expected because PVFORM assumes that the system operates with a maximum power point tracker.

In the development of the program there has been a focus on creating an effective user interface. This is designed to simplify and speed up program operation, and to present output in a form which is useful and illustrative.

Empirical data from monitored photovoltaic systems should be used to verify the simulation program. The program should then be used to assess other simulation and sizing techniques.

The program should be extended to simulate hybrid remote area power supply systems. The modelling of wind, diesel, petrol and hydro powered generators should be considered.

The development of a technique which uses the simulation structure for automatic system sizing should be considered. This might involve the collaborative use of a simple analytical sizing technique, or optimisation through the analysis of the sensitivity of the system to variation of the fundamental parameters.

An economic package should be considered in the further development of PVPro for the assessment of the long-term economic potential of photovoltaic systems. This would enable photovoltaic systems to be compared on an economic basis with other competing systems or with differently configured photovoltaic systems.

The finished product constitutes a meaningful step forward in improved computer simulation of photovoltaic systems.

TABLE OF CONTENTS

LIST OF FIGURES

NOMENCLATURE

AC
Alternating current.

C_b
Battery heat capacity [kJ/kg°C].

DC
Direct current.

ERI
Energy Research Institute.

I_b
Battery current [A].

I_g
Battery gassing current [A].

I_l
Load current [A].

I_{mp}
Maximum power point current [A].

I_{pv}
Photovoltaic module current [A].

INOCT
Installed nominal operating cell temperature: the cell temperature of an installed array at NOCT conditions (800 Wm^{-2} solar irradiance, 20°C ambient temperature and 1 ms^{-1} wind speed), which takes into account the mounting configuration.

I_{sc}
Short circuit current [A].

I-V Curve
Current-voltage curve: a curve which describes the electrical characteristics of a device (current as a function of voltage).

k
Boltzmann's constant: 1.381×10^{-23} [J/K].

LOPP
Loss of power probability: an indication of the expected failure rate of a power supply system in providing the required energy in a particular environment.

M_b
Battery mass [kg].

N_{cb}
Number of cells per battery.

N_{pc}
Number of plates per cell (for a battery).

P_l
Load power [W].

P_{mp}
Maximum power point [W].

PVFORM
A photovoltaic system simulation program for stand-alone and grid-interactive applications developed at Sandia National Laboratories (Menicucci and Fernandez, 1988).

PVPro
A simulation program for stand-alone photovoltaic systems with battery storage developed Energy Research Institute at the University of Cape Town and detailed in this report.

q
Electron charge: 1.602×10^{-19} [C].

Q_{500}
Battery capacity at the 500 hour discharge rate [Ah].

Q_d
Battery capacity for a specified discharge current [Ah].

Q_g
Battery capacity (normalised with respect to Q_{500}) above which gassing occurs.

Q_{pv}
Plane of array irradiance [W/m^{-2}].

Q_t
Battery charge [Ah].

R_b
Battery internal resistance [Ω].

R_l
Characteristic resistance of the load [Ω].

R_{sho}
Shunt resistance [Ω]: this is equal to the absolute value of the inverse of the slope of the photovoltaic I-V curve at I_{sc} (usually determined graphically).

R_{so}
Series resistance [Ω]: this is equal to the absolute value of the inverse of the slope of the photovoltaic I-V curve at V_{oc} (usually determined graphically).

T_{am}
Ambient temperature moving average [°C].

T_b
Battery temperature [°C].

T_{pv}
Photovoltaic cell temperature [°C].

TMY
Typical meteorological year: a set of 8760 hourly weather observations containing actual weather sequences intended to represent the mean long-term climatic conditions for a particular location.

UCT
University of Cape Town.

V_b
Battery voltage [V].

V_{br}
Battery rest voltage [V].

V_{mp}
Maximum power point voltage [V].

V_n
Nominal system voltage [V].

V_{oc}
Open circuit voltage [V].

V_{pv}
Photovoltaic module voltage [V].

$\Delta I_{mp}\Delta Q_{pv}$
Variation of I_{mp} with irradiance [A/Wm^{-2}].

$\Delta I_{mp}\Delta T_{pv}$
Variation of I_{mp} with temperature [A/°C].

$\Delta I_{sc}\Delta Q_{pv}$
Variation of I_{sc} with irradiance [A/Wm^{-2}].

$\Delta I_{sc}\Delta T_{pv}$
Variation of I_{sc} with temperature [A/°C].

$\Delta P_{mp}\Delta Q_{pv}$
Variation of P_{mp} with irradiance [W/Wm^{-2}].

$\Delta P_{mp}\Delta T_{pv}$
Variation of P_{mp} with temperature [W/°C].

$\Delta V_{mp}\Delta Q_{pv}$
Variation of V_{mp} with irradiance [V/Wm^{-2}].

$\Delta V_{mp}\Delta T_{pv}$
Variation of V_{mp} with temperature [V/°C].

$\Delta V_{oc}\Delta Q_{pv}$
Variation of V_{oc} with irradiance [V/Wm^{-2}].

$\Delta V_{oc}\Delta T_{pv}$
Variation of V_{oc} with temperature [V/°C].

CHAPTER 1

INTRODUCTION

1.1 RATIONALE

1.1.1. Economical Sizing

The effectiveness in optimising the sizing of photovoltaic systems economically is a function of the certainty of the sizing technique used. Also, in many situations - especially in non-critical applications in underdeveloped areas - systems should be economically sized for a specified loss of power probability.

Current photovoltaic sizing techniques used by commercial enterprises in South Africa - primarily based on imported software - are believed to be inadequate for economical sizing in this country. They do not incorporate loss of power probability analysis, with its associated versatility, and do not represent system components with sufficient precision.

A computer-based analytical sizing tool has been developed at the Energy Research Institute (ERI) at the University of Cape Town (UCT) which incorporates loss of power probability in the sizing methodology. Precise system simulation provides a means of validating this and the other analytical sizing techniques. Furthermore, it can be used to fine-tune the sizing process and to estimate the long-term performance of monitored systems.

1.1.2. Precision Simulation

Most of the current sizing methods are based on monthly or daily average irradiance or an estimated number of continuous *no sun* days to determine optimal array and battery capacities. However, due to the dynamic nature of photovoltaic systems and the stochastic nature of solar irradiance, such methods are generally inadequate for accurate sizing in developing area situations where affordability is critical.

An hourly simulation program - one which models the performance of a specified system over a year, updating and monitoring the energy flows and states within the system on an hourly basis - provides a suitable framework for more precise system

performance simulation in that each component of the system can be represented more accurately.

Also, a graphical presentation of the hourly variation of the battery state of charge over a simulated year provides a valuable overview of the system performance. It provides an indication, for example, of how the system is coping with the demand and over what periods during the year it is capable of providing too little or too much energy. In addition, it shows how deeply and how regularly the battery is cycled, which facilitates the selection of a battery type with characteristics suitable for a particular system.

Suitable hourly simulation programs are not readily available. It should be noted that what is required is not a sizing program, that is one which is specifically designed to recommend the size of certain system components which would enable a photovoltaic system to meet specified performance criteria under given environmental conditions. Nor is it a simulation model, which is designed to assess the long-term economic potential of a photovoltaic system under specific conditions (which may be used to compare a given photovoltaic system with other competing systems or differently configured photovoltaic systems). As indicated previously, precise system simulation is required for the validation of analytical sizing techniques, for the fine-tuning of the sizing process and for the estimation of the long-term performance of monitored systems.

Two existing programs based on computation of photovoltaic system performance on an hourly basis are discussed in appendix A. The one, developed at the Asian Institute of Technology, is a sizing program and is thus based primarily on fairly simplistic models of the system constituents and inputs. The second, developed at Sandia National Laboratories, is a simulation model and thus designed primarily to assess the long-term economic potential of systems. Although it is constituted by more precise models, it is designed for systems with maximum power point trackers. This is inappropriate for hourly simulation in the Southern African context, where optimum power point trackers are uncommon.

The battery models used in these programs are felt to be inadequate for precision simulation. An ERI project has been undertaken to provide characteristic battery data for improving the accuracy of battery simulation.

1.1.3. Loss of Power Probability

The loss of power probability, LOPP, of a power supply system indicates the system's expected failure rate in providing the required energy in a particular environment. If, for example, a system requires power for six hours per day, a LOPP of 0.01 would mean that the system is likely to fail to meet the demand for twenty-two hours in an average year.

The incorporation of loss of power analysis in a sizing procedure facilitates the design of more affordable systems (increasing the array or battery size for a specified context has a diminishing marginal rate of return on improving the reliability of the system). Systems with perfect reliability are sized to sustain a critical period, which usually occurs only over a very short percentage of time and are hence oversized for most of the time.

Experience derived from current photovoltaic demonstration projects undertaken by the ERI has shown that the potential gains of incorporating LOPP analysis are significant for making photovoltaic systems more affordable in Southern Africa. This is particularly so for systems designed to meet minimal domestic electrical requirements in underdeveloped areas.

1.2 OBJECTIVES

Based on the principles outlined in the preceding discussion, the primary objective of the project is the development of a program for the simulation of stand-alone photovoltaic systems with battery storage.

Utilising site-specific hourly weather data - ordinarily in the form of a typical meteorological year (TMY) - the program is to simulate the dynamics of a user-defined system (including a specified hourly load profile) for one complete year. The loss of power probability of the given system configuration is to be ascertained by computing energy flows on an hourly basis and monitoring the battery state continuously.

The models of the various system constituents and states are to facilitate precision simulation. In addition, they must also accommodate a simpler level of simulation for instances where data describing devices is meagre, or if quicker simulation is required.

For the simulation to deal with photovoltaic systems without maximum power point trackers, it is necessary to determine the operating points of the system components at each hour. This is because all the system components are mutually interactive. To illustrate this concept, consider the simple case of a photovoltaic module charging a battery, with no other system components. The photovoltaic current output is dependent on its voltage, which is the battery voltage, which in turn is dependent on its charge current, that is the photovoltaic current output.

The program is to be developed for use with a microcomputer so that it can be used extensively and can exploit the advantages of such an environment (for example, a well-developed language compiler with advanced features). To facilitate upgrading and modification at a later stage, it is to be coded in an easily maintainable format.

Other existing photovoltaic system modelling programs, such as Solcel-II (Hoover, 1980), Solsys (Edenburn, 1981), E&R (Gonzalez *et al.*, 1982), PV-TAP (Lambarski *et al.*, 1978) and TRNSYS (Evans *et al.*, 1978), are not ideally suitable for this application.

1.3 OVERALL PROCEDURE

In broad terms, the procedure for the formulation of the simulation program was as follows:

- the selection of a suitable programming language,
- the development and coding of the simulation structure,
- the accumulation of empirical data and analytical models of the system elements to be simulated,
- the selection or development of models for these elements
- the coding of these models, and
- the complete debugging of the integrated system.

1.4 CONSTRAINTS

The primary constraint was the time duration of the project. This resulted in a focus on establishing a robust and powerful simulation framework, with an emphasis on a comprehensive algorithm for the interactive solution of the operating points, and modular units for each of the elements modelled to enable easy alteration of them at a later stage.

The program could not be verified with actual photovoltaic system data because adequate data from monitoring sites was not available. Instead, to ensure that the program's predictions are reasonable, a comparison of the simulation performance of the program with that of PVFORM was felt to be adequate.

A constraint which affected the choice, development and implementation of models in the simulation procedure was the program execution time. This was minimised as far as possible without significant loss of precision.

The program was constrained to model a photovoltaic system for one simulated year. To model performance for more than one year, input data can be used which is intended to be representative of the system characteristics or environment over the entire period of interest. Alternatively, the system can be simulated year by year, carrying relevant parameters from one year over to the next.

1.5 SCOPE

The project is confined to the simulation of stand alone photovoltaic systems incorporating the following constituents (see figure 1.1):

- a fixed, flat-plate photovoltaic array (without maximum power point tracking),
- a regulator to prevent overcharging of the battery,
- a battery bank,
- a load shed device to prevent discharge of the battery beyond its design capacity,
- an inverter, and
- AC and DC loads.

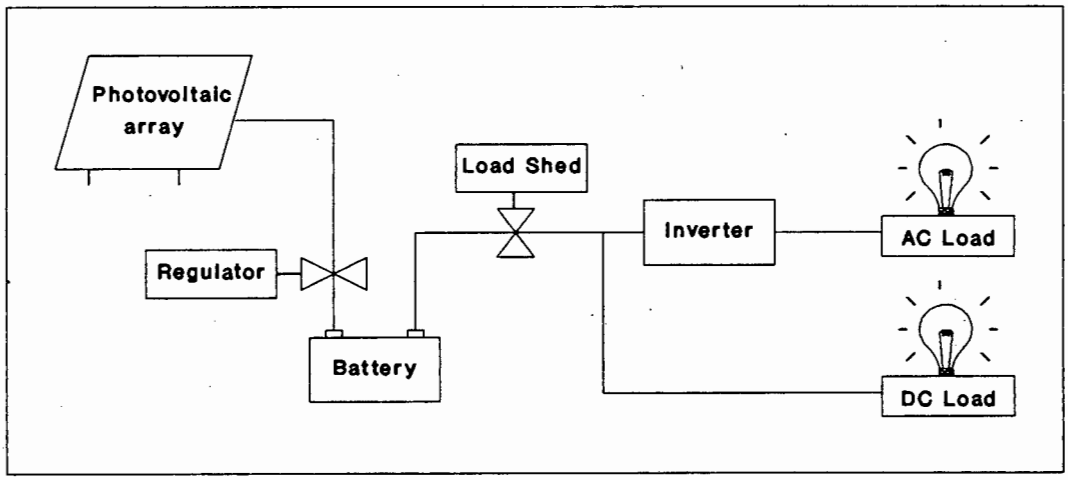

Figure 1.1 System diagram

1.6 REPORT OUTLINE

This report commences with a description of the structure of the simulation program, called PVPro. In particular, the computer language, the modular structure, the level of modelling complexity and the user interface are described.

The subsequent section deals with the modelling of the system state: the weather data as input, the plane-of-array irradiance model, the photovoltaic cell temperature model and the battery temperature model.

Next is a section on the system component models. These include the photovoltaic module current, the regulator efficiency and voltage, the battery current and voltage, the inverter efficiency, the load shed voltage and the load current.

After that, the entire procedure for calculating the system operating point is discussed. This section covers interactive curve solving, constraints of hourly simulation approximation, an improved hourly simulation method, load shed approximations, the numerical root solving method, the I-V limit specification, and details of the implementation of the operating point calculation.

Program outputs are described in the next section. In particular the graphical output and the summarised and detailed data files are discussed.

Finally, conclusions are drawn from the findings of the project and recommendations are made.

The full listing of the program coding is not included in this report because of its length.

CHAPTER 2

PROGRAM STRUCTURE

This section describes the structure of the computer program and the principles which directed its development. It begins with the computer coding medium. Next the structure of the coding is dealt with, then the level of modelling complexity and finally the user interface.

2.1 COMPUTER LANGUAGE

Turbo Pascal was selected as the medium for the development of PVPro for the following considerations:

- it is used extensively and is thus well-supported (hence the source code is more likely to be easily accessible to users),
- it facilitates a structured and modular programming approach, which improves the maintainability of the coding,
- it accommodates the development of sophisticated user-friendly interfacing between the computer and the end user,
- it offers support for various complex routines such as curve fitting and high speed screen writing, and
- its compiler is well-developed and thus generates efficient coding with a fast execution speed.

2.2 MODULAR STRUCTURE

PVPro has been coded in a modular structure, with each of the system elements modelled in a separate and hence easily maintainable unit. Data characteristic of each of these elements is stored in its corresponding unit. This is particularly important concerning the updating or the modification of models at a later stage.

2.3 LEVEL OF MODELLING COMPLEXITY

A dominant feature of PVPro is versatility in the level of modelling complexity, which is determined by the availability of the input data or the required level of precision.

Either default algorithms, based on fundamental attributes of the various system components, or default generic empirical characteristics are provided for simple modelling. If accurate empirical data describing components is accessible, it can be used to enhance the precision of the simulation.

If the program execution time is significant, simple models should be selected to enhance the simulation speed. This may be especially pertinent in the initial stages of a system sizing procedure.

2.4 USER INTERFACE

User-friendliness is regarded as an important aspect of making the program accessible to all users - simple and speedy program operation being the primary objective.

Pull-down menus were selected as the most suitable means of setting up a system structure for simulation. They facilitate exceedingly fast selection of options and the presentation of a great deal of information with few key strokes. A fast screen writing procedure is used to display the menus.

Routines used to acquire input data from the user are also designed to simplify this process as far as possible.

During the simulation procedure, the current julian day, battery depth of discharge and number of load shed hours are displayed. The depth of discharge is displayed graphically if the program is run on a system with a standard graphics adapter. These parameters provide a valuable portrayal of the system performance.

CHAPTER 3

SYSTEM STATE MODELLING

This section describes the methodology used to determine the basic environmental conditions under which the photovoltaic system operates. It starts with the primary input required - weather data - and then details the models used to calculate the plane-of-array irradiance, the photovoltaic cell temperature and the battery temperature.

3.1 WEATHER DATA INPUT

3.1.1. Hourly Data Sets

The weather data is input as a set of hourly values for an entire 365-day year comprising ambient temperature, wind speed, and global and diffuse irradiance.

3.1.2. Typical Meteorological Year

In using an hourly simulation program such as PVPro for sizing purposes, the weather data is often, although not necessarily, input in the framework of a typical meteorological year (TMY). A TMY incorporates hourly weather observations containing actual weather sequences that are intended to represent the mean long-term climatic conditions for a particular location.

A concise review of the literature related to the generation of TMY data sets is contained in Pissimanis *et al.* (1988) and details of the methodology used for this project are contained in appendix B.

The following meteorological parameters were used in the selection of *representative* data (with their associated weightings in brackets):

- the daily maximum value (0.0889), minimum value (0.0222), mean (0.0445) and range (0.0111) of the wind speed,
- the daily maximum value (0.1754), minimum value (0.0175), mean (0.1053) and range (0.0351) of the ambient temperature, and
- the total daily global (0.2500) and direct irradiance (0.2500) - the direct irradiance being calculated from the total daily global and diffuse irradiance.

The parameter weightings were selected according to their estimated relative significance in determining the photovoltaic system state. They are similar to those specified in Pissimanis *et al* (1988).

TMYs have been generated for the following South African sites:

Name	Grade
Cape Town	A
Durban	A
Port Elizabeth	A
Alexander Bay	B
Keetmanshoop	B
Bloemfontein	C
Pretoria	C
Upington	C
Windhoek	C

The grading is a rough measure of the size of the weather data base which was used to generate the TMY. Grade A TMYs are based on approximately twenty years of data, grade B on about fifteen years and grade C on less than 12 years of data.

PVPro requires diffuse irradiance as one of its inputs. This parameter has been measured by the Weather Bureau on an ongoing basis only at its primary stations in South Africa and Namibia, located at twelve centres. Of these twelve centres, the nine listed above contained adequate weather data for the generation of TMYs, but the data for the other three was insufficient.

3.2 PLANE-OF-ARRAY IRRADIANCE MODEL

The plane-of-array (POA) irradiance - the irradiance incident on a tilted photovoltaic array - consists of the following three components: direct beam, sky diffuse and ground-reflected irradiance (refer to Hay and McKay, 1985, and Liu and Jordan, 1963, for details).

Calculation of the direct component is relatively straightforward using the geometrical relationships between this parameter, the direct normal irradiance and the solar incidence angle on the tilted surface.

The ground-reflected component is substantially smaller than the others. In view of this and for simplicity, the reflection component is assumed to source isotropically from an infinite horizontal surface in front of the tilted plane. This isotropic ground-reflected irradiance model is used widely because it is adequate for those surfaces common to photovoltaic applications (such as grass or gravel surfaces, as opposed to water and snow surfaces).

The sky diffuse component is the largest potential source of computational error and can be modelled either isotropically or anisotropically. The isotropic model is simple in that it assumes a uniform diffuse irradiance intensity over the entire sky dome. It provides a good fit to empirical data at low intensity overcast conditions, but underestimates diffuse irradiance at high solar intensities common to clear or partly clear sky situations.

The anisotropic model developed by Perez *et al.* (1987) incorporates the effects of increased diffuse irradiance near the sun and near the horizon. Their most recent version of the model (used in PVFORM) is widely-accepted and well-established. This model has been implemented in PVPro, based on the coding of the model in PVFORM. The coding in PVFORM was found to result in computational anomalies at sunrise and sunset and was modified for PVPro (consequently this correction has also been implemented in a new version of PVFORM).

These models require the following inputs to calculate the POA irradiance:

- the site latitude,
- the hemisphere in which the site is located,
- the albedo of the surface in front of the array,
- hourly horizontal global irradiance levels, and
- hourly horizontal diffuse irradiance levels.

3.3 PHOTOVOLTAIC CELL TEMPERATURE MODEL

The photovoltaic cell temperature model used in PVFORM and developed by Fuentes (1987) has been implemented in PVPro. This thermal model requires a minimum of input and has been found experimentally to have an error of less than 5°C.

The model, being iterative, calculates an initial approximation of the cell temperature and then uses this estimation to formulate a closer approximation. This process is repeated until the difference between the current estimate and the previous one is within a specified tolerance. This tolerance is stipulated by the user and has a range of 0.1°C to 1°C.

The model requires the following inputs to calculate the cell temperature:

- hourly POA irradiance levels,
- hourly ambient temperature levels,
- hourly wind speed levels,
- the array height above ground, and
- the installed nominal operating cell temperature (INOCT).

3.4 BATTERY TEMPERATURE MODEL

The battery temperature is estimated primarily by calculating the moving average of the ambient temperature for a specified interval prior to the current hour of simulation. This provides a means of specifying how immediate the effect of the ambient temperature is on the battery temperature. For example, the temperature of a battery located in a position with little environmental protection would follow the ambient temperature fairly closely and a small interval would be stipulated for the simulation. On the other hand, a large interval would be appropriate for a battery placed in a well insulated environment which would be affected only by long term variations in the ambient temperature.

The internal heating effect due to current flow within a battery is also taken into account in approximating the battery temperature. The temperature increase resulting from the battery current of the preceding hour is added to the base battery temperature determined by the ambient temperature (the heat generated inside a battery during an hour is assumed to dissipate during the following hour).

The battery temperature is thus estimated as follows:

$$T_b = T_{am} + 3.6 \times (I_{b'} - I_{g'}) \times (V_{b'} - V_{br'}) / (M_b \times C_b)$$

where:

C_b = battery heat capacity [kJ/kg°C],
I_b = battery current [A],
I_g = battery gassing current [A],
M_b = battery mass [kg],
T_{am} = ambient temperature moving average [°C],
T_b = battery temperature [°C],
V_b = battery voltage [V], and
V_{br} = battery rest voltage [V].

(variables marked with a dash are those from the previous hour)

The model requires the following inputs:

- the battery voltage, rest voltage and current from the previous hour,
- hourly ambient temperature levels,
- the battery mass, and
- the battery heat capacity.

CHAPTER 4

SYSTEM COMPONENT MODELLING

This section describes the models of the system elements. The photovoltaic module model is described first, then the regulator, the battery, the inverter, the load shed unit and finally the load.

4.1 PHOTOVOLTAIC MODULE CURRENT MODEL

PVPro is based on interactive I-V curve modelling. This necessitates that the user either utilises a default model for the photovoltaic I-V curve that is based on a few typical module parameters, or provides empirical I-V curve data.

4.1.1. Analytical Model

A number of photovoltaic I-V curve models were considered, and a model based on the one outlined in Rauschenbach (1980) was selected for implementation in PVPro (refer to appendix C for details of the evaluation).

This model requires the following input data:

- the open circuit voltage, short circuit current and maximum power point voltage and current for a base I-V curve at a specified POA irradiance level and cell temperature, and
- the variation of these parameters with POA irradiance and cell temperature, assumed linear.

The following method is used to calculate the photovoltaic current output, for a given voltage, POA irradiance and cell temperature:

$$I_{sc} = I_{sco} + \Delta I_{sc}\Delta Q_{pv} \times (Q_{pv} - Q_{pvo}) + \Delta I_{sc}\Delta T_{pv} \times (T_{pv} - T_{pvo})$$
$$V_{oc} = V_{oco} + \Delta V_{oc}\Delta Q_{pv} \times (Q_{pv} - Q_{pvo}) + \Delta V_{oc}\Delta T_{pv} \times (T_{pv} - T_{pvo})$$
$$I_{mp} = I_{mpo} + \Delta I_{mp}\Delta Q_{pv} \times (Q_{pv} - Q_{pvo}) + \Delta I_{mp}\Delta T_{pv} \times (T_{pv} - T_{pvo})$$
$$V_{mp} = V_{mpo} + \Delta V_{mp}\Delta Q_{pv} \times (Q_{pv} - Q_{pvo}) + \Delta V_{mp}\Delta T_{pv} \times (T_{pv} - T_{pvo})$$

$$C_2 = (V_{mp} / V_{oc} - 1) / \text{Ln} (1 - I_{mp} / I_{sc})$$
$$C_1 = (1 - I_{mp} / I_{sc}) \times \text{Exp} (-V_{mp} / C_2 / V_{oc})$$
$$I_{pv} = I_{sc} \times (1 - C_1 \times (\text{Exp} (V_{pv} / C_2 / V_{oc}) - 1))$$

where:

I_{mp} = maximum power point current [A],
I_{pv} = photovoltaic module current [A],
I_{sc} = short circuit current [A],
Q_{pv} = plane of array irradiance [Wm^{-2}],
T_{pv} = photovoltaic cell temperature [°C],
V_{mp} = maximum power point voltage [V],
V_{oc} = open circuit voltage [V],
V_{pv} = photovoltaic module voltage [V].
$\Delta I_{mp}\Delta Q_{pv}$ = variation of I_{mp} with irradiance [A/Wm^{-2}],
$\Delta I_{mp}\Delta T_{pv}$ = variation of I_{mp} with temperature [A/°C],
$\Delta I_{sc}\Delta Q_{pv}$ = variation of I_{sc} with irradiance [A/Wm^{-2}],
$\Delta I_{sc}\Delta T_{pv}$ = variation of I_{sc} with temperature [A/°C],
$\Delta V_{mp}\Delta Q_{pv}$ = variation of V_{mp} with irradiance [V/Wm^{-2}],
$\Delta V_{mp}\Delta T_{pv}$ = variation of V_{mp} with temperature [V/°C],
$\Delta V_{oc}\Delta Q_{pv}$ = variation of V_{oc} with irradiance [V/Wm^{-2}], and
$\Delta V_{oc}\Delta T_{pv}$ = variation of V_{oc} with temperature [V/°C].

(variables suffixed by an 'o' refer to the base I-V curve data)

The model was tested by comparing modelled I-V curves with empirical curves of a variety of modules over their full voltage ranges at various irradiance and temperature levels. The worst deviation of the modelled curves from the original curves was usually for voltages near the average of the maximum power point voltage and the open circuit voltage. Errors at the worst points on most curves were about two to ten percent, with errors of usually less than three percent over the remaining portion of the curves.

Worst case errors for the base curves were up to about thirteen percent for a few modules. For the curves derived from these base curves for other irradiance and temperature levels, the errors were up to about seventeen percent at the worst sections of the curves, and up to about three percent for the remainder of the curves.

The effect of this error on the overall simulation depends on the simulation configuration and environment. If the system operating point is often in the near-vertical portion of the photovoltaic I-V curve, then the overall simulation precision is

likely to be affected significantly (eight to fifteen percent). This could happen in very hot climates (high cell temperatures tend to reduce the maximum power point and open circuit voltages), or with panels that have relatively low maximum power point and open circuit voltages, or with batteries that have a relatively high charging voltage. If, on the other hand, the system is designed to operate below or at the maximum power point, the error is likely to be far less significant (one to four percent).

4.1.2. Empirical Data

The use of empirical I-V curves provides a means of improving the precision of the photovoltaic simulation procedure. PVPro has been designed to facilitate the use of such data, with an independent program being used to process the raw I-V curve data into a format suitable for the main simulation system.

Normally I-V curve data is available in the form of one set of I-V curves for a range of irradiance levels at a fixed temperature and a second set for a range of cell temperatures at a fixed irradiance. Data which indicates the combined effects of temperature and irradiance on the I-V curves is not usually accessible, and therefore such effects are assumed to be independent.

a. Overall Approach

Empirical photovoltaic I-V curve data is provided in the form of two sets of I-V curves (refer to figure 4.1 for an example of typical data). The first set is a family of curves at various POA irradiance levels and at a fixed cell temperature level, the second set a family of curves at various cell temperature levels and at a fixed POA irradiance level. One of the curves is common to both sets.

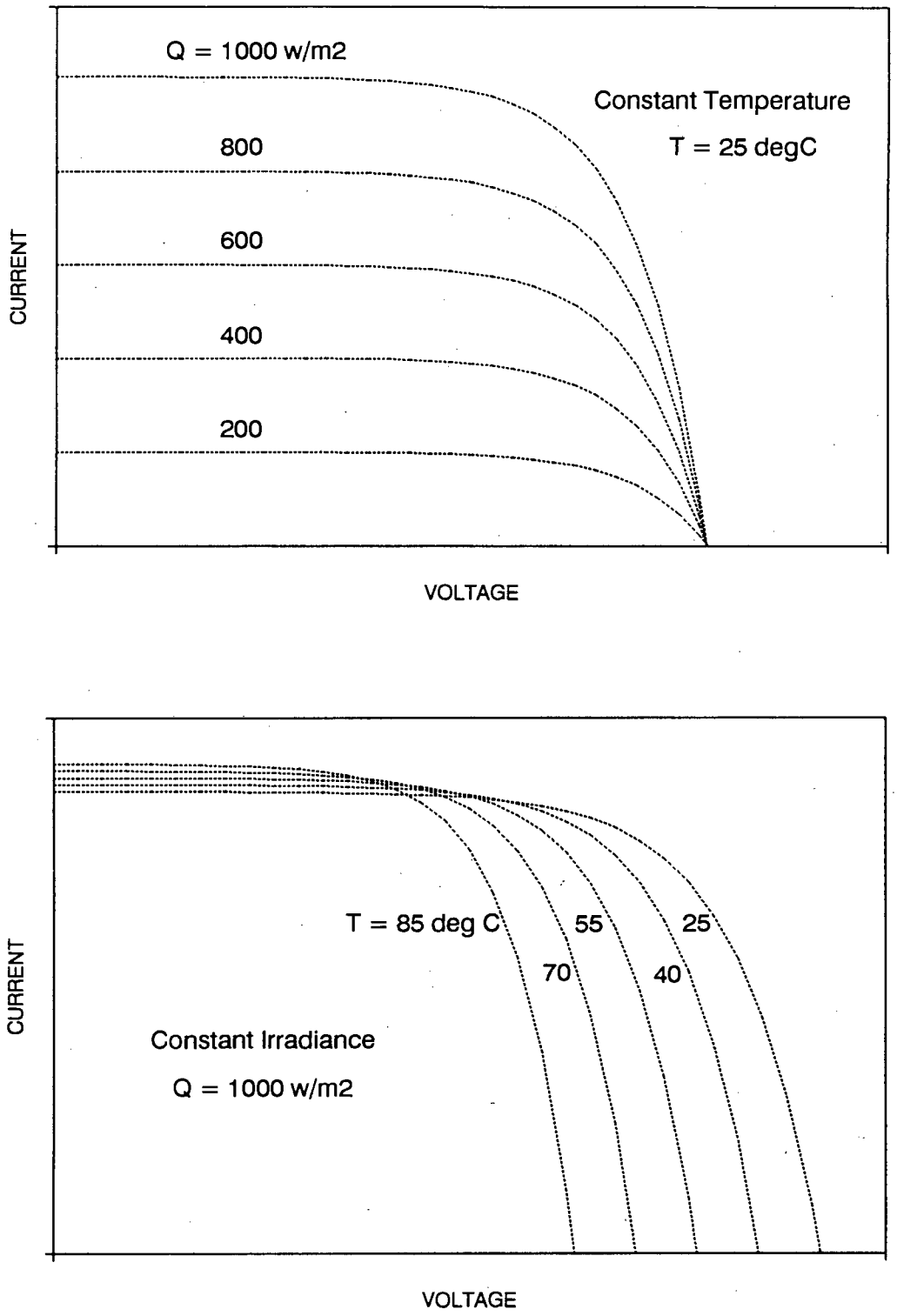

Figure 4.1 Typical empirical photovoltaic I-V curve data

PVPro is structured in such a way that the photovoltaic model is required to calculate the photovoltaic current in response to a given voltage, irradiance and cell temperature:

$$I_{pv} = fn\ (V_{pv}, Q_{pv}, T_{pv})$$

where:

I_{pv} = photovoltaic module current [A],
V_{pv} = photovoltaic module voltage [V],
Q_{pv} = plane of array irradiance [Wm^{-2}], and
T_{pv} = photovoltaic cell temperature [°C].

A feasible way of implementing this process using empirical I-V curves is based on interpolation between the curves supplied to find the essential point on the I-V curve for the specified irradiance and temperature.

Interpolation is implemented along constant v lines, where v is the voltage at any point on a curve divided by the open circuit voltage for that curve (refer to figure 4.2). These lines of interpolation are selected for pragmatic reasons: they result in a simple numerical implementation method and allow the use of the full set of original data curves for each interpolation (interpolation along constant voltage lines would, for example, result in the exclusion of curves whose open circuit voltage is less than the voltage under consideration).

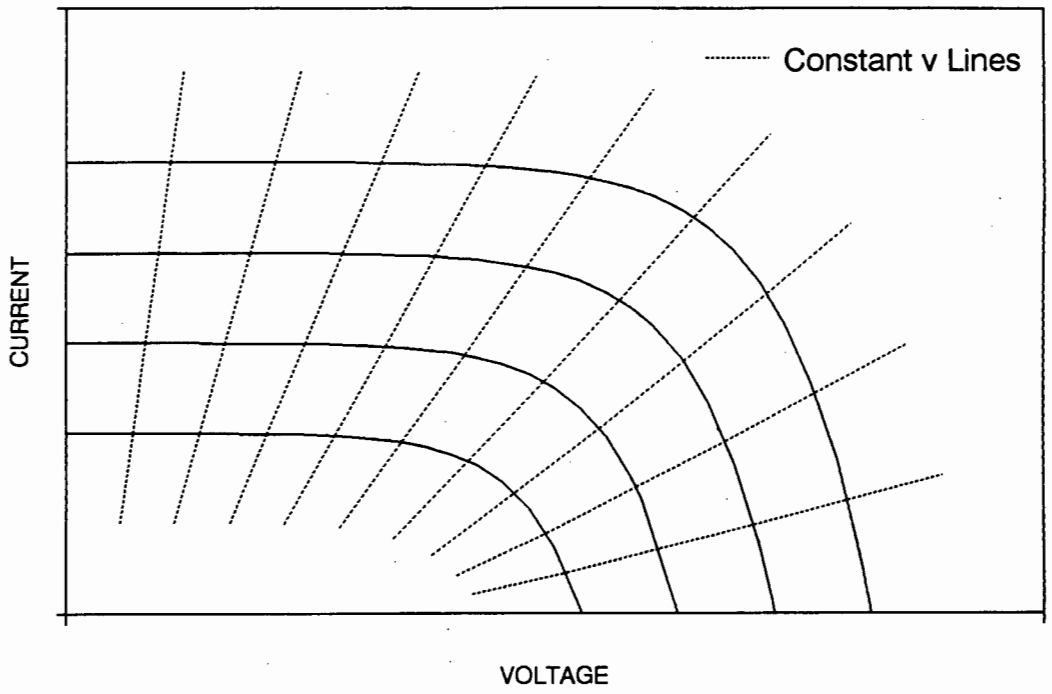

Figure 4.2 Illustration of constant v lines for a typical set of I-V curves

To simplify the explanation of the methodology for calculating the photovoltaic current for a specified voltage, irradiance and temperature, consider the case of calculating the current at 12 volts for an irradiance of 800 Wm^{-2} and a cell temperature of 65°C ($I_{pv\ 12\ 800\ 65}$). The input data consists of two sets of I-V curves: one at a constant cell temperature of 25°C and the other at a constant irradiance of 1000 Wm^{-2}.

The first step in calculating the photovoltaic current for a specified voltage is the calculation of the open circuit voltage of the I-V curve at the designated temperature and irradiance ($V_{oc\ 800\ 65}$). Interpolation between the open circuit voltages of the family of input I-V curves at constant temperature is used to calculate the open circuit voltage of the I-V curve at the specified irradiance, but at the input data temperature ($V_{oc\ 800\ 25}$). Refer to figure 4.3.

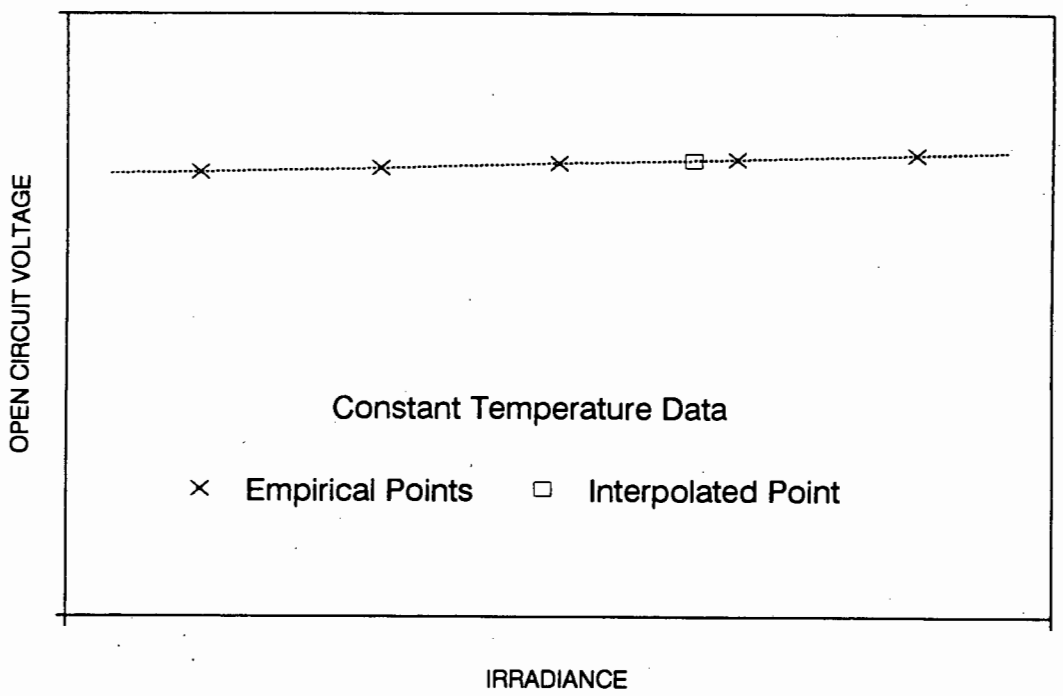

Figure 4.3 Interpolation of open circuit voltage with constant temperature data set

Then similar interpolation on the constant irradiance data set is used to determine the open circuit voltage of the I-V curve at the specified temperature, but at the input data irradiance ($V_{oc\ 1000\ 65}$). See figure 4.4.

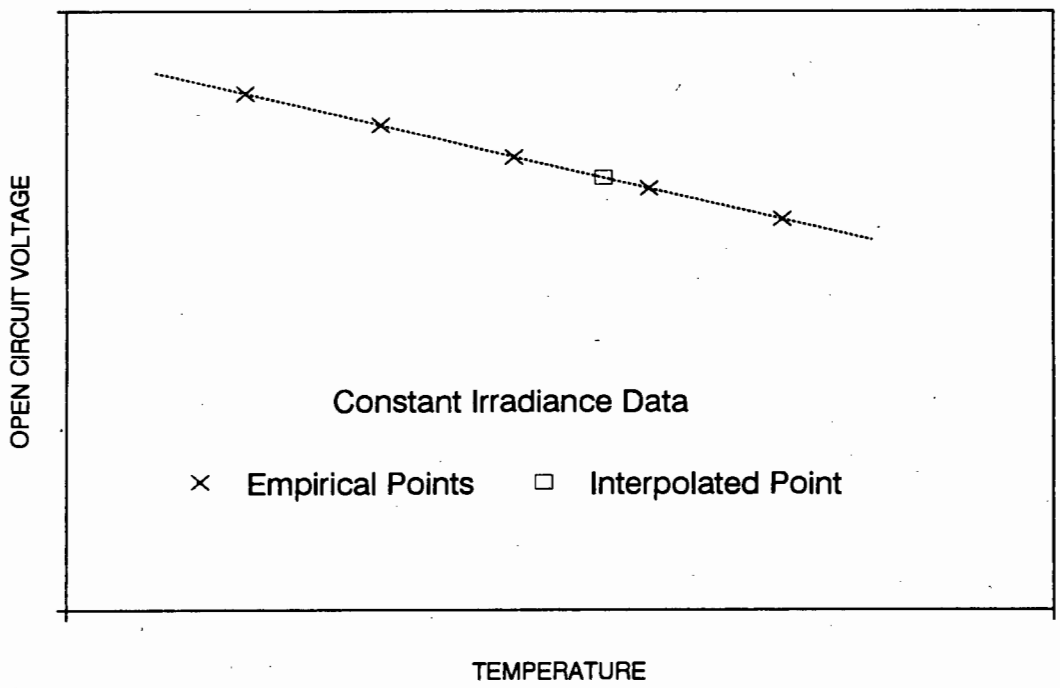

Figure 4.4 Interpolation of open circuit voltage with constant irradiance data set

The open circuit voltage for the curve common to both families of curves ($V_{oc\ 1000\ 25}$) is subtracted from this to determine the variation in open circuit voltage caused by the difference in temperature between the specified temperature and the temperature of the constant temperature input curves ($\Delta V_{oc\ 1000\ 25\text{-}65} = V_{oc\ 1000\ 65} - V_{oc\ 1000\ 25}$). The final open circuit voltage is thus calculated by adding the voltage caused by the temperature difference to the voltage at the specified irradiance ($V_{oc\ 800\ 65} = V_{oc\ 800\ 25} + \Delta V_{oc\ 1000\ 25\text{-}65}$).

The specified voltage at which the photovoltaic current output is to be determined is divided by this open circuit voltage to calculate the appropriate value of v at which to effect interpolation ($v = 12 / V_{oc\ 800\ 65}$).

The next step is to calculate the current output at the required irradiance level and at the input data cell temperature ($I_{pv\ v\ 800\ 25}$). This is done by interpolation between the I-V curves provided at various irradiance levels along the constant v line, as illustrated in figure 4.5.

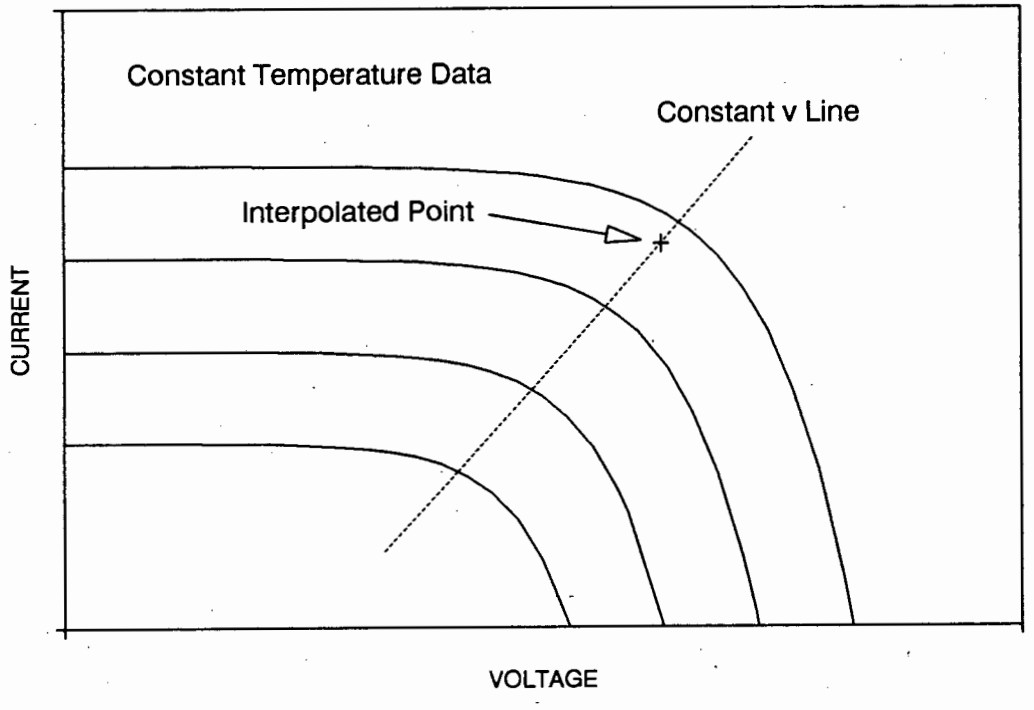

Figure 4.5 Interpolation along constant v line with constant temperature data set

The temperature effect is considered next. Again it is assumed that the effect of this parameter on the I-V curves can be determined by interpolation along constant v lines. Thus, for the given voltage parameter v, the current output at the required temperature level and at the input irradiance ($I_{pv\ v\ 1000\ 65}$) is calculated. The current on the curve common to both families of curves ($I_{pv\ v\ 1000\ 25}$) is subtracted from this to determine the variation in current caused by the difference in temperature between

the specified temperature and the temperature of the constant temperature input curves ($\Delta I_{pv\ v\ 1000\ 25\text{-}65} = I_{pv\ v\ 1000\ 65} - I_{pv\ v\ 1000\ 25}$). Refer to figure 4.6.

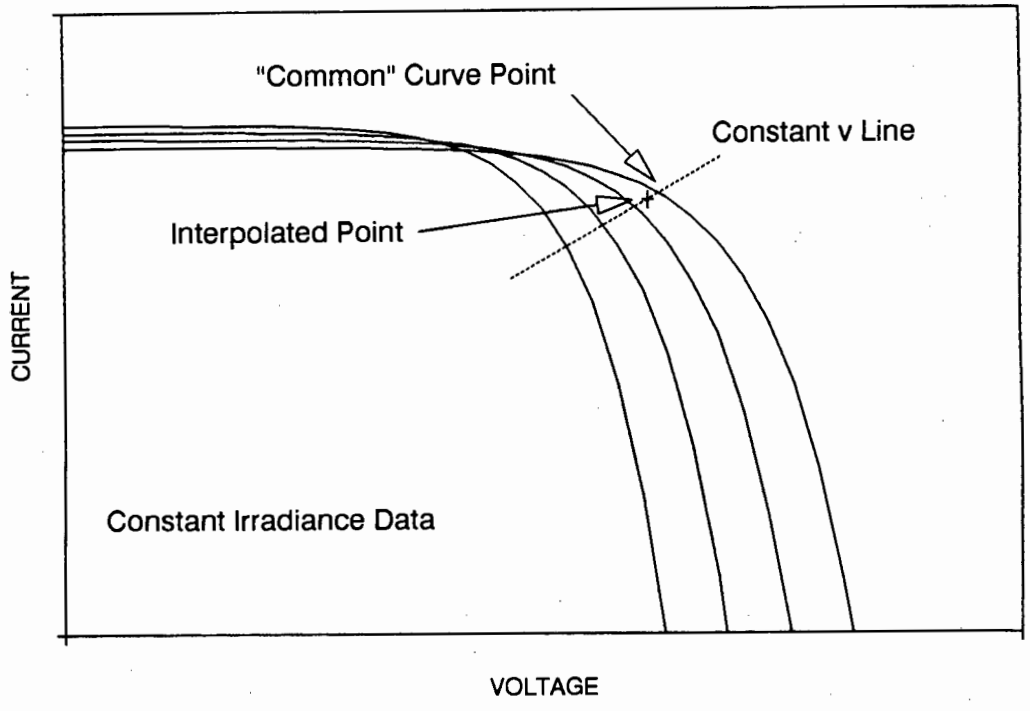

Figure 4.6 Interpolation along constant *v* line with constant irradiance data set

This current difference is added to the current calculated previously for the specified irradiance level to yield the photovoltaic current at the required irradiance and temperature level ($I_{pv\ 12\ 800\ 65} = I_{pv\ v\ 800\ 25} + \Delta I_{pv\ v\ 1000\ 25\text{-}65}$).

b. Input Data Processing

To simplify the implementation of the interpolation procedure in the simulation routine described above, the original input data is preprocessed in a separate program to generate a large number of I-V curves which then constitute the input data for PVPro. Thus, for each of the two families of I-V curves (one at constant temperature and varying irradiance and the other at constant irradiance and varying temperature), a new family of curves is generated with a very small interval (of the varying parameter) between curves. Because the intervals between curves are small, interpolation can be performed linearly between adjacent curves without significant loss of precision (as opposed to sophisticated interpolation using a large number of interpolating curves). This process, in effect, fits an approximated surface to the input data and decreases the processing time during simulation.

The source data consists of a number of sets of voltage - current points, with one set describing each I-V curve. The first step in the preprocessing procedure is the normalisation of this source data along the voltage axis (that is, for each data set every voltage data point is divided by the open circuit voltage for that curve). This facilitates the use of the data in the system based on normalised voltages described above (interpolation along constant v lines).

Next a smooth curve, in the form of a cubic spline interpolant, is fitted to each of the normalised source data sets (approximating the shape of the original I-V curve associated with that set, as shown in figure 4.7). The cubic spline method is used at this stage because it generates a curve very close to the original curve by fitting a cubic polynomial to the interval between each pair of data points. The resulting curve passes through every data point, is continuous, has continuous first and second derivatives, and at both data endpoints has its second derivative equal to zero (this makes it a *free* cubic spline).

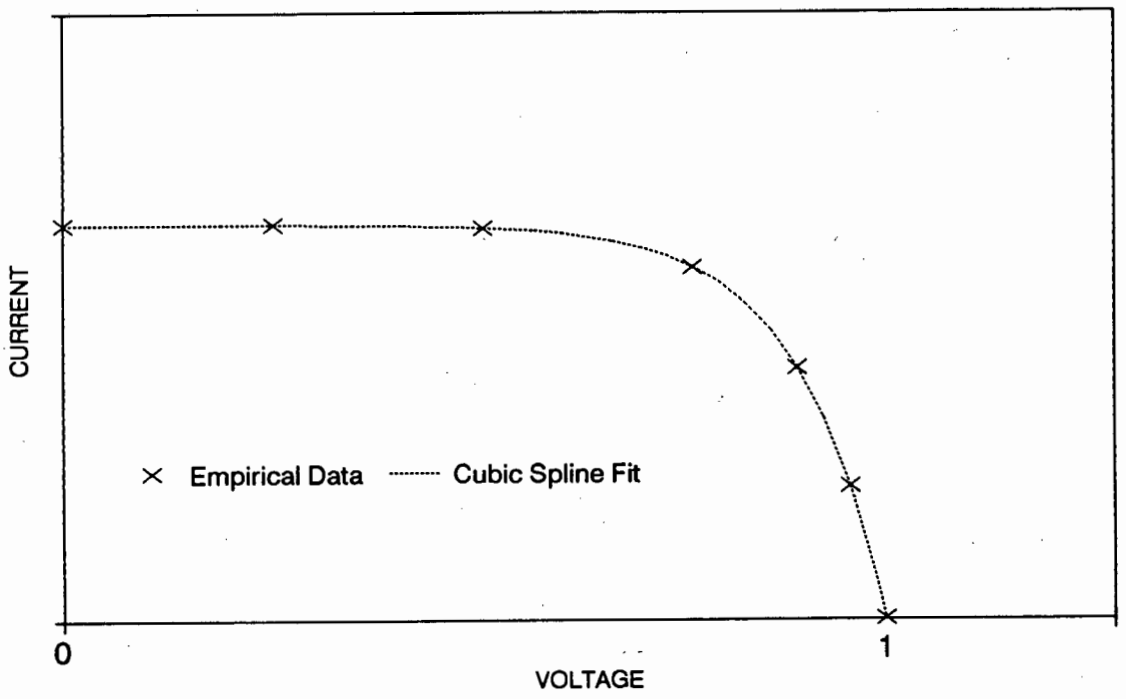

Figure 4.7 Cubic spline fit on normalised empirical data

Simultaneous to the generation of the cubic splines, data points are yielded along these fitted curves. These points are used to fit constant v lines at a later stage (as shown in figure 4.8) and are calculated at v intervals of 0.1 from 0.1 to 0.5, and of 0.02 from 0.52 to 1. There are as many intervals as can be processed easily, with smaller intervals over the near-vertical segments of the curves.

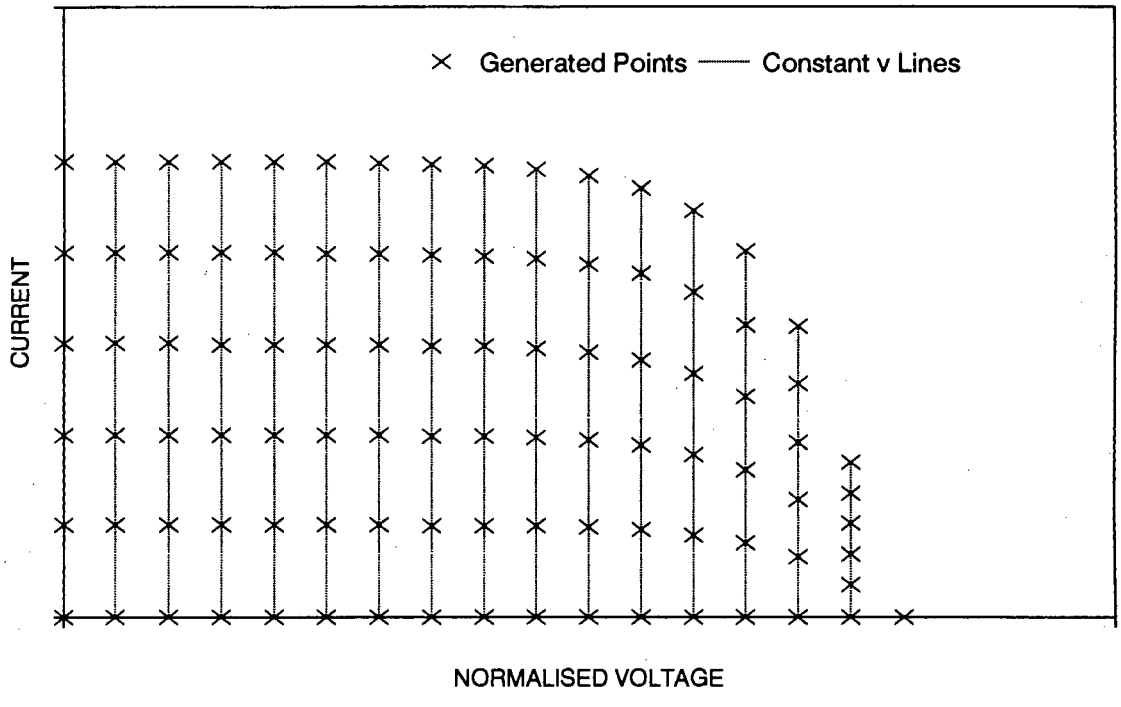

Figure 4.8 Illustration of constant v lines used in data massaging

The next operation is the subtraction of each of the temperature I-V curves from the base temperature I-V curve (the curve which is common to both families of curves). That is, for each constant v point the current of the base temperature curve is subtracted from the current of the curve being massaged.

Then a cubic spline is fitted to the open circuit voltage data of both families of curves (this data must be retained because the curves are normalised with respect to voltage). Again, simultaneous to this process, a large number of data points are generated along these two curves. Ninth order polynomials are fitted to the data by least squares approximation. The reason for fitting a cubic spline to the original data and generating extra points before fitting a polynomial to the data is that high order polynomials (greater than about five) have a tendency to oscillate wildly if fitted to an insufficient number of data points. Using a large number of data points and the least squares method prevents such an oscillatory response. The least squares approach is useful in that it allows the specification of the order of polynomial to be fitted independent of the number of data points and hence the accurate description of a curve by a few coefficients.

Cubic spline curves are then fitted to the constant v data points generated earlier (when processing the irradiance curves, the voltage axis is added as an extra I-V curve for zero irradiance). Concurrently, data points are generated along these curves to be used to fit a set of curves at a variety of constant irradiance and temperature levels.

After this, cubic spline curves are fitted to these generated data points at constant parameter (irradiance or temperature) levels, as shown in figure 4.9. A large set of data points along each of these curves is produced. Eleventh order polynomials are fitted to these sets of points by the least squares method, the coefficients of which form the basis of the input data for PVPro.

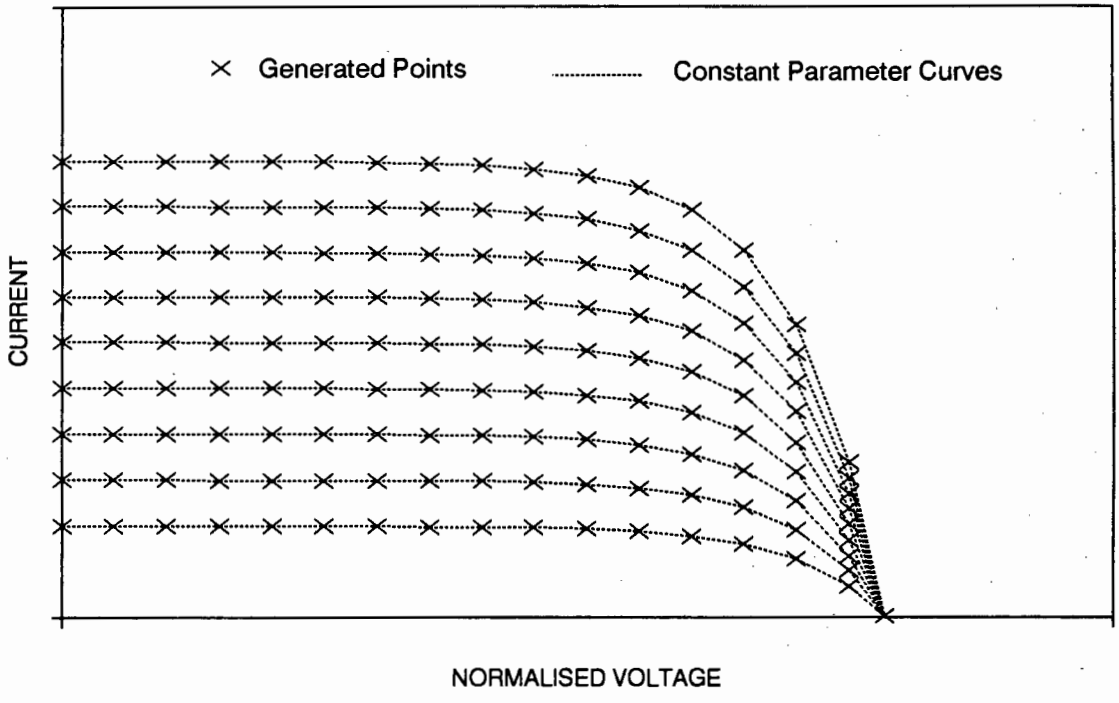

Figure 4.9 Illustration of constant parameter curves used in data massaging

A number of fitted and interpolated I-V curves were compared with the original data. The deviation of the modelled curves from the original curves was consistently within one percent over most of each curve. The worst deviation (in percentage terms) was usually for voltages near the open circuit voltage, where the current levels involved are considerably smaller. Errors in this region were normally in the order of five to ten percent, but in absolute terms were very small (and the system is not expected to operate in this section for much of the time). The effect of this error on the overall simulation is not substantial.

Polynomial functions are fitted to each of the new curves, which are thus represented by a small set of coefficients (details follow in the next section). Curves are generated at irradiance levels between 0 and 1350 Wm^{-2} at 30 Wm^{-2} intervals, and at temperature levels between 0 and 135°C at 3°C intervals.

4.2 REGULATOR EFFICIENCY AND VOLTAGE MODEL

Regulator models suitable for interactive photovoltaic system modelling were not available. Hence a generalised regulator model, which can be applied to a broad range of devices, has been implemented. The model can be used to characterise either specific regulators or generic regulator types. In this model, a regulator is described by its voltage drop and its current efficiency.

The voltage-current curve of the regulator (voltage across the device as a function of current flowing through it) is assumed to be a straight line. The user specifies the slope of this curve (in effect, the resistance of the device) and the voltage axis intercept (the voltage drop at zero current). The voltage drop modelled in this way is not intended to represent the regulating voltage which is characteristic of certain devices, but only the voltage drop which occurs across the device when it is permitting normal current flow.

The current efficiency of the device is defined as the current that flows from the regulator to the battery divided by the current that would pass from the photovoltaic array to the battery were the regulator not included in the system. This component of the model is used primarily, but not exclusively, to specify the regulating characteristic of the device.

The current efficiency is represented by two series of straight lines plotted on a graph as a function of the battery voltage (refer to figure 4.10). The model initially uses the first series which describes the efficiency up to a specified battery voltage set point. If the battery voltage increases above that point, the second set of curves is used. This set describes the efficiency down to a specified battery voltage, and when the battery voltage drops below this point, the first set is used again, and so on. This process allows hysteresis in the device to be modelled.

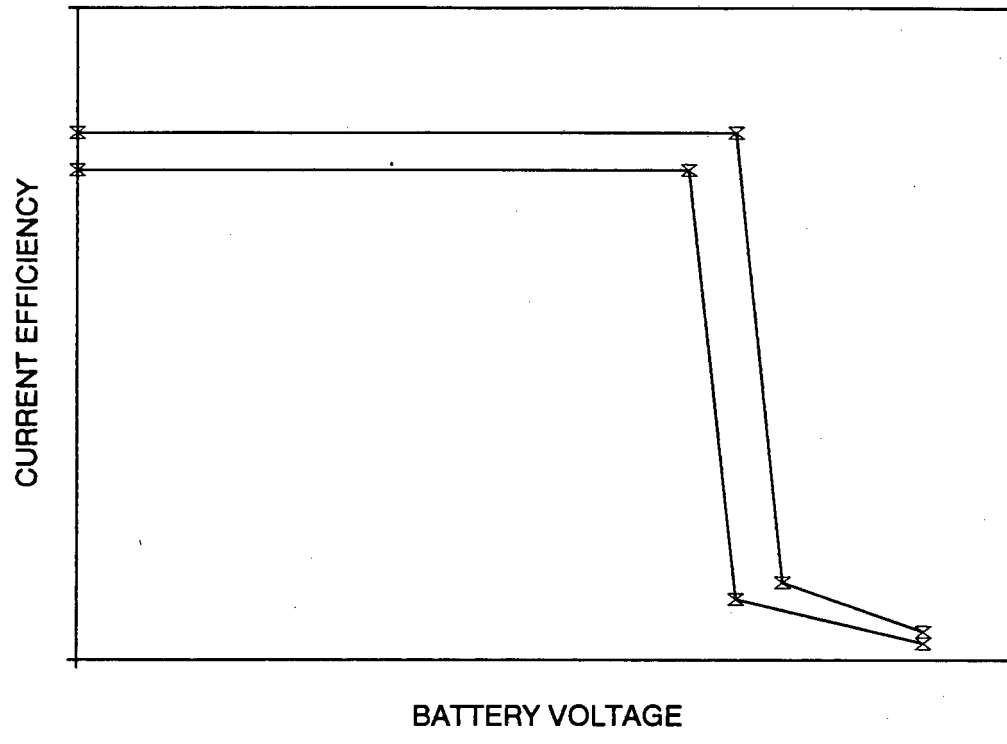

Figure 4.10 Current efficiency specification

Consider, for example, a transistor-based boost / float regulating device (constant voltage regulation). The voltage drop across the device when it is not regulating would be modelled linearly as described above. The first set of the current efficiency curves would consist of two sections. The first section might consist of a nearly horizontal efficiency line at a high efficiency level from zero battery voltage up to a specified voltage (the boost or float voltage). The second section would be a vertical curve at this voltage, since the regulator would not allow any current to flow to the battery above this voltage. If the device incorporated hysteresis, the second set of the current efficiency curves would be identical in form to the first, but with a lower cut-off voltage.

A second example is a relay-based device, which switches off the current flow once a second for a tenth of a second to measure the battery voltage (representing a ten percent loss of photovoltaic array energy). If the battery voltage increases above a certain setpoint, the device starts regulating by switching off the current periodically for one second over a four second interval. Gradually this duty cycle is decreased as the voltage increases until no current flows through the device. There is no significant voltage drop across the device, so the coefficients used to model this characteristic would be set to zero. The representation of both current efficiency curves would be similar in form and would consist of two or more sections. The first section might consist of a horizontal efficiency line at an efficiency of approximately

ninety percent (the duty cycle of the device when it is not regulating) up to the voltage at which regulation commences. The second and additional sections would be curves that characterise the reduction of efficiency from about ninety percent to zero percent over the specified battery voltage range. The efficiency in this section would approximate the duty cycle of the device.

4.3 BATTERY CURRENT AND VOLTAGE MODEL

The interactive curve solving algorithm requires a model which generates battery I-V curves (illustrated in figure 4.11) for a specified depth of discharge (and temperature, if required). Such a model must evaluate the battery current for a stipulated voltage. In addition, models are required to calculate the battery rest voltage and the battery gassing current.

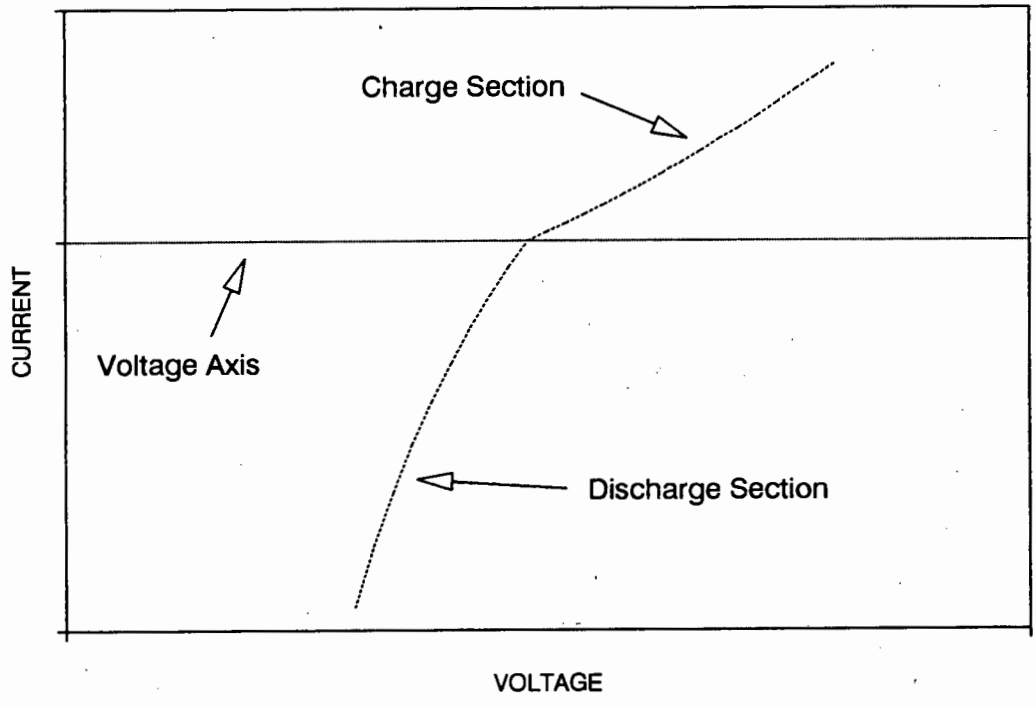

Figure 4.11 Illustrative battery I-V curve

PVPro incorporates an analytical, a generic and an empirical battery model. To characterise a battery, the analytical model requires few battery parameters as input and is the simplest level of modelling. The generic model is more sophisticated and requires as input a set of voltage curves as a function of battery depth of discharge for different current levels. Each set describes a generic battery type (such as traction or

standby-tubular batteries, for example). The empirical model also requires such sets of curves, but furthermore requires these curves for a range of battery temperatures.

The overall procedure for representing the battery I-V curves for a specified battery depth of discharge (and temperature, if necessary) is common to all the models. Approximate curves are fitted to the battery curve data, with separate curves for charge and discharge I-V curves, as required. The curves are fitted from the voltage axis, with their current range being specified by a minimum current boundary for discharge curves and a maximum boundary for charge curves.

Cubic spline curves are used to approximate the I-V curves over the appropriate current range. This is done by dividing the current range into convenient intervals, calculating the voltage at the borders of these intervals and fitting the splines to the resulting I-V points. A cubic polynomial function is thus used to approximate the battery curve over each interval.

The splines are fitted as a function of v, where v is the voltage difference between the voltage at the point of interest and the minimum voltage over the current range, multiplied by a factor of one hundred. This is done because the battery I-V curves are generally very steep and thus ill-suited for curve fitting (the independent variable intervals are too small).

The splines are characterised by sets of coefficients (a set of four coefficients for each of the intervals) and a list of the interval boundaries. Such a data set is then used to calculate the battery current for a given voltage (this process thus being independent of the original battery model).

The cubic spline method does have two disadvantages. Firstly, a large number of coefficients are required to characterise the fitted curve. Secondly, when calculating the fitted function value for a given argument, the interval in which that argument lies must first be determined to establish which set of coefficients to use.

Nevertheless, cubic splines are used for this application because they provide a close fit with relatively few data points. To attain the same level of accuracy from a polynomial fit, a high order polynomial would be required. With few original data points, such a function would tend to become oscillatory, especially for steep curves as are characteristic of battery I-V curves. In addition, splines can be fitted to any reasonable number of data points, which enables this system to manage varying amounts of user-supplied data (for the generic and empirical models).

4.3.1. Analytical Model

The implementation of the I-V curve fitting procedure based on the analytical battery model requires the selection of current values, within the specified current range, at which to determine the I-V points used in constructing the cubic spline fit. Five current values are specified for each of the charge and discharge curves.

The one boundary value is set at zero current and the other at a hundred and ten percent of the stipulated minimum (for a discharge curve) or maximum (for a charge curve) boundary current. The three intermediate points are spaced such that the interval between two points is fifty percent larger than the corresponding interval immediately closer to the voltage axis. Therefore, the density of points increases close to the voltage axis. This improves the accuracy of the curve fitting, which is based on free cubic splines, since the derivative of the slope of the battery I-V curve also increases close to the voltage axis.

The following model, based on few input parameters, is used to approximate the battery rest voltage, the battery voltage for a given current and the battery gassing current:

$$V_{br} = (2.15 - 0.18 \times (Q_{500} - Q_t) / Q_{500}) \times N_{cb}$$

For charging ($I_b > 0$):

$$R_b = ((1.125 + (1.5 \times Q_t / Q_{500})^4) / Q_{500}) \times N_{cb}$$
$$V_b = V_{br} + I_b \times R_b + 1.672 \times 10^{-1} \times \ln (10 \times I_b + 1)$$

For discharging ($I_b < 0$):

$$Q_d = Q_{500}^2 / (Q_{500} - I_b \times 1440 \times N_{pc} / Q_{500})$$
$$R_b = (((0.125 + ((Q_{500} - Q_t) / Q_d)^4) / Q_d) \times 100 / Q_{500}) \times N_{cb}$$
$$V_b = V_{br} + I_b \times R_b - 1.338 \times 10^{-1} \times \ln (-10 \times I_b + 1)$$

if $Q_t > Q_d$ then

$$V_b = 0$$

For $I_b > 0$ and $Q_d > Q_g$:

$$I_g = I_b \times (Q_t / Q_{500} - Q_g) / (1 - Q_g)$$

where:

I_b = battery current [A],
I_g = gassing current [A],
N_{cb} = number of cells per battery,
N_{pc} = number of plates per cell,
Q_{500} = battery capacity at the 500 hour discharge rate [Ah],
Q_d = battery capacity (for a specified discharge current) [Ah],
Q_g = battery capacity above which gassing occurs (normalised with respect to Q_{500}),
R_b = battery resistance [Ω],
V_b = battery voltage [V], and
V_{br} = battery rest voltage [V].

This model requires the following input data:

- the battery capacity at the 500 hour discharge rate,
- the battery capacity above which gassing occurs,
- the number of cells per battery, and
- the number of plates per cell.

Details relating to this analytical battery model are contained in Purcell (1990). It was formulated after consideration of a number of models identified via a literature search, of which one was selected to form the basis of this model. Modifications to the underlying model were based on empirical analysis to improve precision especially at low current levels.

4.3.2. Generic Data

The generic model is based on sets of empirical curves used to characterise different battery types. Each of these sets consists of curves of battery voltage as a function of depth of discharge for a range of current levels. An illustrative set is shown in figure 4.12.

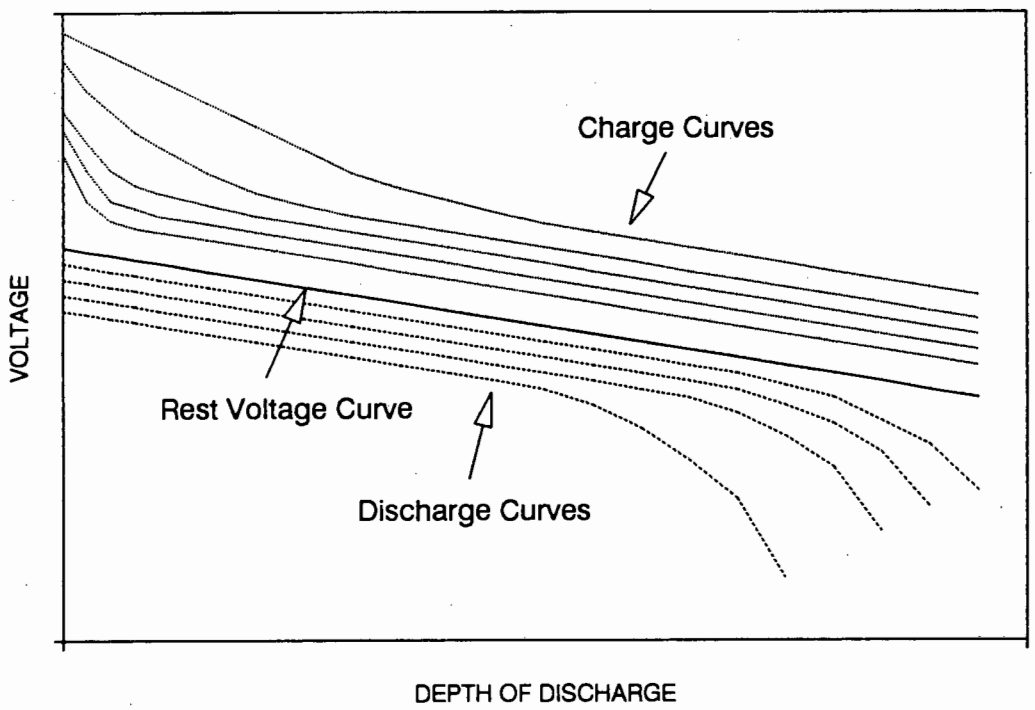

Figure 4.12 Typical empirical battery input data

A peripheral program is used to preprocess the input data to provide data suitable for the main program. The original input data for a battery type is constituted by sets of points on each of the voltage - depth of discharge curves: one set for each current level. Free cubic spline interpolation is implemented on this data to generate a large number of points on each of the curves.

A seventh order polynomial is then fitted by least squares approximation to the points that fall between zero and twenty-five percent of the maximum depth of discharge of the particular curve. Similarly, another seventh order polynomial is fitted to the points that are between fifteen and a hundred percent of the maximum depth of discharge. The first polynomial is used to describe the portion of the curve between zero and twenty percent of the maximum depth of discharge, and the second

the remainder of the curve. The overlapping of the curves in the approximation process is to minimise the discontinuity between fitted curves.

Splitting the curve into two portions thus was found to be the most accurate way of representing the curves. A single polynomial fit was found to be unsuitable for the charge curves, which usually tend to be curved at low depths of discharge and fairly straight over the remainder of the curve.

Curves of gassing current as a function of battery voltage are also generated at this stage. At zero depth of discharge, all charging current is assumed to be gassing current and hence gassing current curves are formed by the battery I-V points at this depth of discharge (gassing current was found experimentally to be largely independent of depth of discharge (Purcell, 1990)). Free cubic spline interpolation is used on the appropriate zero depth of discharge I-V points on the input data curves to generate an extensive number of points on the gassing current curves. A fifth order polynomial is then fitted to these points to characterise the curve.

The main program thus requires a set of coefficients to describe each of the input battery curves. In the implementation of the I-V curve fitting procedure during simulation, based on the generic battery model, the current levels at which I-V points are calculated are determined by the current levels of the input data curves. Input data curves for all current levels from zero up to current level just beyond the minimum or maximum stipulated boundary current are used (with a minimum of three).

The corresponding voltage points are calculated using the polynomial coefficients (as a function of depth of discharge) provided by the preprocessing program. Clamped cubic splines are fitted to the resultant data points (*clamped* splines have their first derivatives at the endpoints of the whole interval specified). The slope of the splines where they intersect the voltage axis is specified as zero. At the other end of the splines, the first derivative is approximated by the slope of the straight line passing through the boundary data point and the data point at the next greater absolute current level available. If the boundary data point is the maximum absolute current level, then this point and the next smaller absolute current level are used.

4.3.3. Empirical Data

The methodology for implementing the model based on empirical data is identical to that for generic data, except that temperature effects are also incorporated. The input data is constituted by a set of empirical curves used to characterise each battery. Each of these sets consists of curves of battery voltage as a function of depth of discharge for a range of current levels and, at each current level, for a range of battery temperatures.

The original input data for a battery is thus constituted by sets of points on each of the voltage - depth of discharge curves: one set for each current level at a particular battery temperature. A peripheral program is used to preprocess the input data in a way similar to that for the generic data curves to provide data suitable for the main program (including the generation of gassing current curves as a function of battery voltage and temperature).

In the implementation of the I-V curve fitting procedure during simulation, based on the empiric battery model, the calculation of voltage levels for specified current levels incorporates the battery temperature effects. Thus, for a given current level, the battery voltage is calculated by interpolation between the curves provided for that current level at different temperatures. Interpolation is between points at constant depth of discharge using Lagrange's interpolary method. This fits a polynomial to the data points (to the order of one less than the number of input data points) and is used here because there are few data points (resulting in a stable low order polynomial). The algorithm is fast.

4.4 INVERTER EFFICIENCY MODEL

The characteristics of inverters are so device-dependent that it was decided to base the efficiency model on empirical data. This allows accurate modelling of the device if data is available. Alternatively, characteristic curves that describe generic categories of devices can be established (general characteristic curves can be specified, for example, for sinusoidal wave inverters, square wave inverters, ferroresonant inverters, et cetera).

A curve of the device efficiency, as a function of the fraction of full load (referred to as the load fraction), is used to describe a particular inverter or an inverter type. Data points on this curve are provided to a peripheral program which generates data suitable for the main program. A tenth order polynomial curve is fitted to the points

(using the method described previously of fitting a cubic spline to the data to generate a large number of points suitable for a high order polynomial least squares fit).

If the user does not define a point for a load fraction of zero, a straight line curve from the origin to the efficiency level at the first user-defined point is used in PVPro itself to describe the efficiency over this range. The input data for PVPro therefore consists of the minimum load fraction which has been specified by the user and a set of eleven coefficients which describes the efficiency curve beyond that minimum fraction.

The maximum power rating of the inverter is specified in the main simulation program itself and is used to calculate the load fraction for each hour during the simulation.

4.5 LOAD SHED VOLTAGE MODEL

PVPro requires two voltage specifications to characterise the load shed unit. The first is the voltage level at which the unit sheds the load (the *down* voltage) and the second the voltage level at which the load is switched back into the system after a load shed occurrence (the *up* voltage). These are specified in the main program itself.

4.6 LOAD CURRENT MODEL

4.6.1. Load Specification

a. Hourly Load Profile

As part of the load specification, PVPro requires an hourly load power profile - either recurrent on a daily or weekly basis (referred to as daily and weekly profiles respectively) or specified for the entire year (an annual profile). For a system with both AC and DC loads, these loads are defined as independent load profiles and comprise separate files.

An autonomous program has been developed to facilitate load profile specification. It provides an editor for the formulation of daily (twenty-four hour) profiles. These daily profiles are used as the basic building blocks for the weekly or annual profiles. A user can, for example, specify a weekly load profile representative of a summer

load and then apply this profile to the whole summer period simply by highlighting the appropriate period.

b. Electrical Characteristics

The load specification also incorporates a simple description of its electrical characteristics. Loads can be specified as being either constant power or constant resistance loads. Loads such as electronic devices fall into the constant power category, in that their power consumption is largely independent of their operating voltage for the normal battery voltage operating range. Other loads have a decreasing power consumption for a decreasing operating voltage and are classified as constant resistance loads. More complex load characteristics, such as those of certain electric motors, are not supported and have to be approximated by either constant power or constant resistance characteristics. These fall outside of the scope of the project.

4.6.2. Load Current Calculation

The load profile of each julian day in the simulation is calculated at the start of that day. The appropriate DC and AC daily load profiles (in power terms) are determined from the daily, weekly or annual profile data. The DC load profile is added to the AC load profile, modified by the inverter characteristic, to compute the total daily load profile.

During the actual hourly simulation process, the load current is solved as follows:

For a load shed condition:

$I_l = 0$

For a constant resistance load:

$R_l = V_n^2 / P_l$
$I_l = V_b / R_l$

(or $I_l = 0$ for $P_l = 0$)

For a constant power load:

$$I_l = P_l / V_b$$

where:

I_l = load current [A],
P_l = load power [W],
R_l = characteristic resistance of the load [Ω],
V_b = battery voltage [V], and
V_n = nominal system voltage [V].

The model requires the following input data:

- the hourly load power,
- the nominal system voltage, and
- whether the load is characterised as a constant resistance or as a constant power load.

CHAPTER 5

SYSTEM OPERATING POINT CALCULATION

5.1 INTERACTIVE CURVE SOLVING

PVPro calculates energy flows on a simulated hourly basis and must therefore calculate the system operating voltage at least hourly (voltage is essential since maximum power point operation is not assumed). Because the voltage and current of the various system elements are mutually dependent (especially between the battery and photovoltaic array), the equilibrium operating voltage of the system has to be located to determine the system state. This is accomplished by a numerical interactive curve solving method.

The battery is treated as the central element of the system because of its dominance in determining the system state (battery voltage establishes the load shed and voltage regulation conditions). The battery voltage is thus designated the system operating voltage, with the photovoltaic array voltage being the sum of the battery and the regulator voltages, and the load voltage being equal to the battery voltage.

To make the system solvable, it is assumed that there is a unique battery I-V curve for a given battery depth of discharge and temperature (and thus at any given instant in time). Also, there is a particular photovoltaic I-V curve at any moment in time (dependent on the POA irradiance and photovoltaic array cell temperature), and a specific load I-V curve (dependent on the electrical characteristics and the nominal power rating of the load). These are illustrated in figure 5.1.

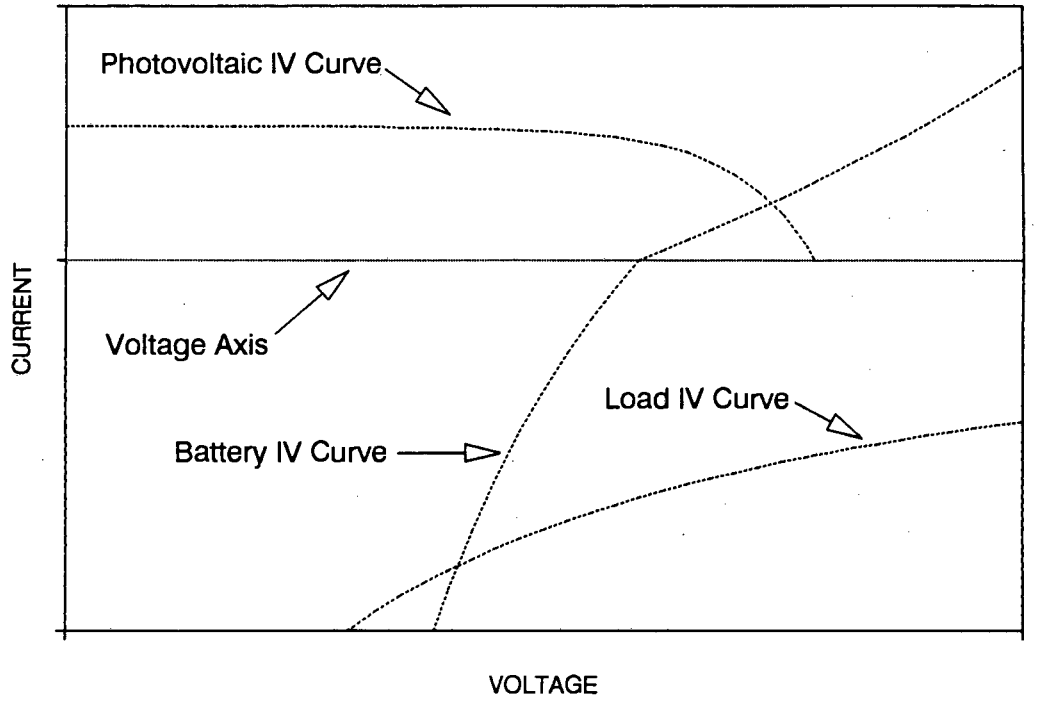

Figure 5.1 Photovoltaic system I-V curves

The nett current flowing into the battery is equal to the regulator output current plus the load current (battery charging current is defined as positive, hence the load discharge current is negative). Thus the intersection of the battery I-V curve with the photovoltaic I-V curve (modified by the regulator characteristics) plus the load I-V curve marks the operating point at any instant in time, as shown in figure 5.2. It is at this battery voltage that the current from the regulator plus the current drawn by the load equals the nett current flowing into the battery. In the figure, the label *Photovoltaic (modified by regulator)* refers to the I-V curve of the photovoltaic array measured at the output of the regulator.

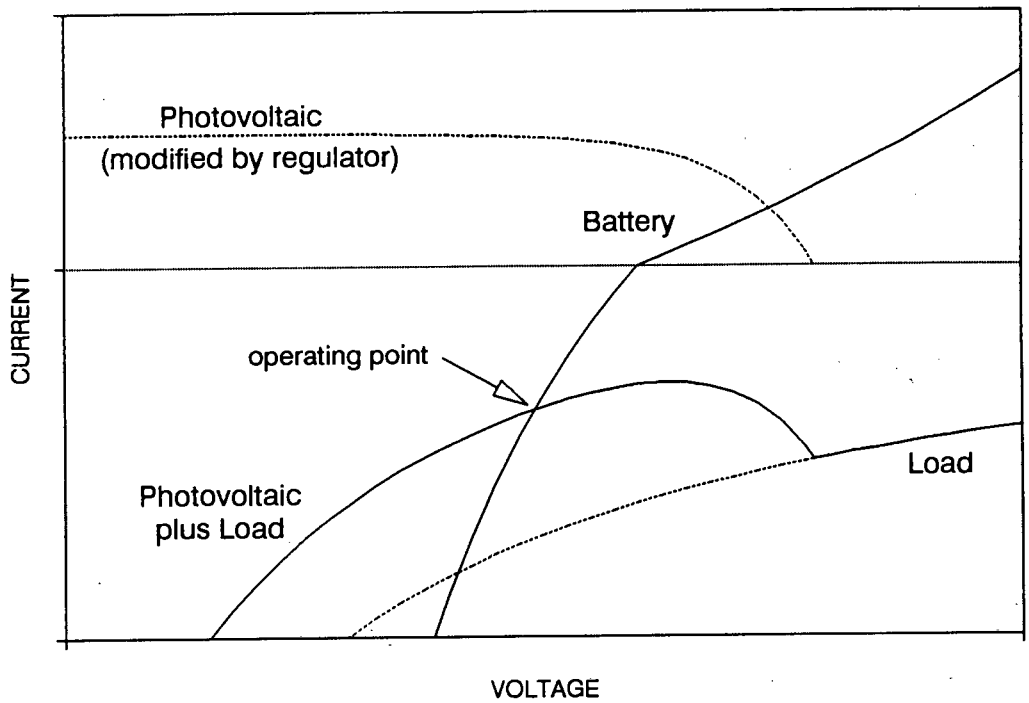

Figure 5.2 System I-V curves showing operating point

5.2 CONSTRAINTS OF HOURLY SIMULATION APPROXIMATION

The input weather data is provided on an hourly basis. Hence the photovoltaic I-V curve is assumed to be constant over the whole hour, based on the average weather data for that hour. Similarly, the load is assumed to be constant over the hour and its I-V curve is also fixed for the hour. This imposes limitations on the accuracy of the simulation, as illustrated in the ensuing example.

For a given hour, assume that the actual irradiance varies during the hour such that the resulting photovoltaic I-V curves are represented by the curves A to C in figure 5.3 (cell temperature and regulator effects are ignored in this example). Assume also that curve A is operative for the first ten minutes of the hour, curve B during the next ten minutes, curve C for the following twenty minutes, curve B again for the next ten minutes and curve A again during the last ten minutes. Lastly, assume that curve B represents the photovoltaic I-V curve for the average irradiance level of the hour and that the load is constant throughout the hour.

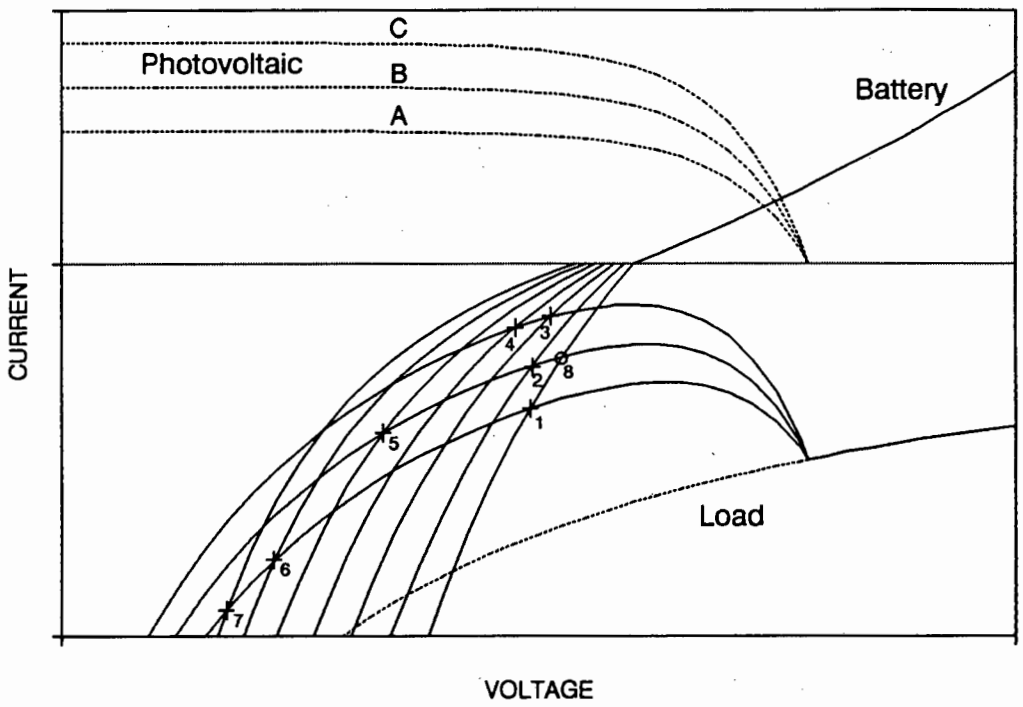

Figure 5.3 Approximation of hourly operating point locus

Points 1 to 6 indicate the system operating points for the start of each ten minute interval within the hour and point 7 the operating point at the end of the hour. Point 1 is the intersection between the battery curve at the start of the hour and the load curve plus curve A. This point falls in the battery discharge region (negative current below the voltage axis) and as the battery discharges the battery I-V curve shifts to the left during the first ten minute interval (the battery I-V curve is largely dependent on its depth of discharge and shifts to the left while discharging).

Point 2 indicates the intersection between the new battery I-V curve and the photovoltaic / load I-V curve at the start of the second ten minute interval (modification of the battery curve in the charging region is not shown in this diagram). Similarly, points 3 to 6 indicate remaining operating points during the hour and point 7 the operating point at the end of the hour. The operating point locus for the hour would pass through these points.

However, within an hourly simulation framework, the only available information at the start of each hour is the battery I-V curve at that instant and the photovoltaic I-V curve which would result from the average irradiance level for the hour (curve B in

this case). The intersection of these curves is at point 8, which could represent an inadequate approximation of the operating point locus for the case outlined above.

There is no straightforward process to improve this estimation as far as the variation of the photovoltaic I-V curve during the hour is concerned. However, the approximation can be improved by using a more appropriate battery I-V curve than the one at the start of the hour for the operating point calculation.

5.3 IMPROVED HOURLY SIMULATION METHOD

As indicated previously, the I-V curve information available at the start of each simulation hour is the photovoltaic I-V curve for the mean hourly irradiance, the battery I-V curve for the beginning of the hour and the load I-V curve. Of these, the photovoltaic and load I-V curves remain constant throughout the hour, but the battery I-V curve does shift during the hour (see figure 5.4).

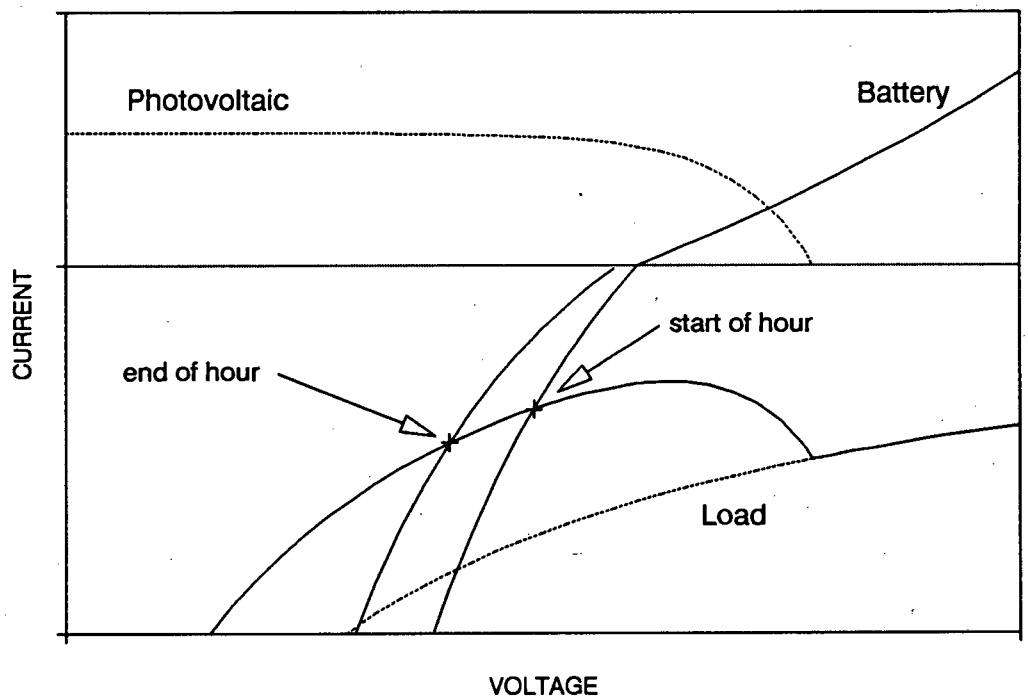

Figure 5.4 I-V curves at start and end of hour

Solving for the operating point using this data available at the start of the hour yields an approximation of the operating current and voltage only for the start of the hour.

Ideally, the average operating voltage and current point for the hour should be located and a simple method of approximating this point is outlined below.

The operating current for the start of the hour (i_s in figure 5.5) is calculated using interactive curve solving. This current is used to estimate a projected battery depth of discharge for the end of the hour and a corresponding battery I-V curve is generated. An operating current (i_e) and voltage (v_e) for this new battery state is calculated, and the ultimate mean operating current (i_m) is approximated by the average of i_s and i_e (only current is considered at this stage, since the average current is used to calculate the battery depth of discharge at the end of the hour and the average voltage is not used).

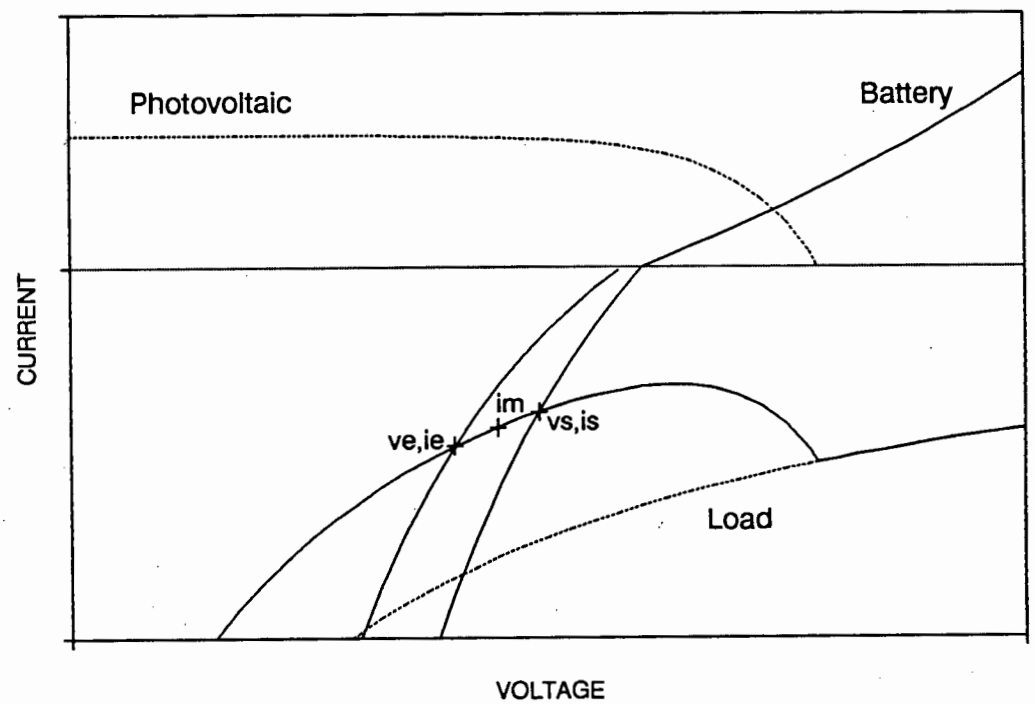

Figure 5.5 Improved simulation operating points

5.4 LOAD SHED APPROXIMATIONS

The load shed status of the system is determined by two load shed voltage levels. The first is the voltage at which load shedding occurs for a system which has been operating in the operative (no load shed) state. The second is the voltage at which the system reverts to the operative state after a load shed condition.

For simplicity, once a load shed situation has arisen during an hour it is assumed to prevail until the end of the hour. In practice, when a load shed situation does arise the system is unlikely to revert to normal operation within a short period of time and the impact of such an assumption on overall simulation accuracy is expected to be minimal.

The system load shed status is fundamental to the operating point calculation procedure. With regard to this, there are three possible system scenarios during an hour:

- the operating voltage at the start of the hour is in the load shed region,
- the operating voltage at the start and at the end of the hour are both in the operative region, and
- the operating voltage at the start of the hour is in the operative region but falls in the load shed region at the end of the hour.

In the first scenario, with the initial operating point in the load shed region, the system remains in load shed state for the entire hour. In the second scenario, with both starting and ending operating points in the operative region, the system is in operative mode for the whole hour.

However, the third scenario involves a change in the load shed status of the system during the hour, with the system starting in the operative region at the beginning of the hour but ending in the load shed region. In this case, it is necessary to calculate the battery depth of discharge at the point of load shed (refer to figure 5.6). This could be done by finding the battery depth of discharge that results in a battery discharge I-V curve which interacts with the photovoltaic / load I-V curve at the load shed voltage. In practice this process is not feasible since it would require excessive computer time (battery I-V curves would have to be generated at a number of depth of discharge levels until the correct one was identified).

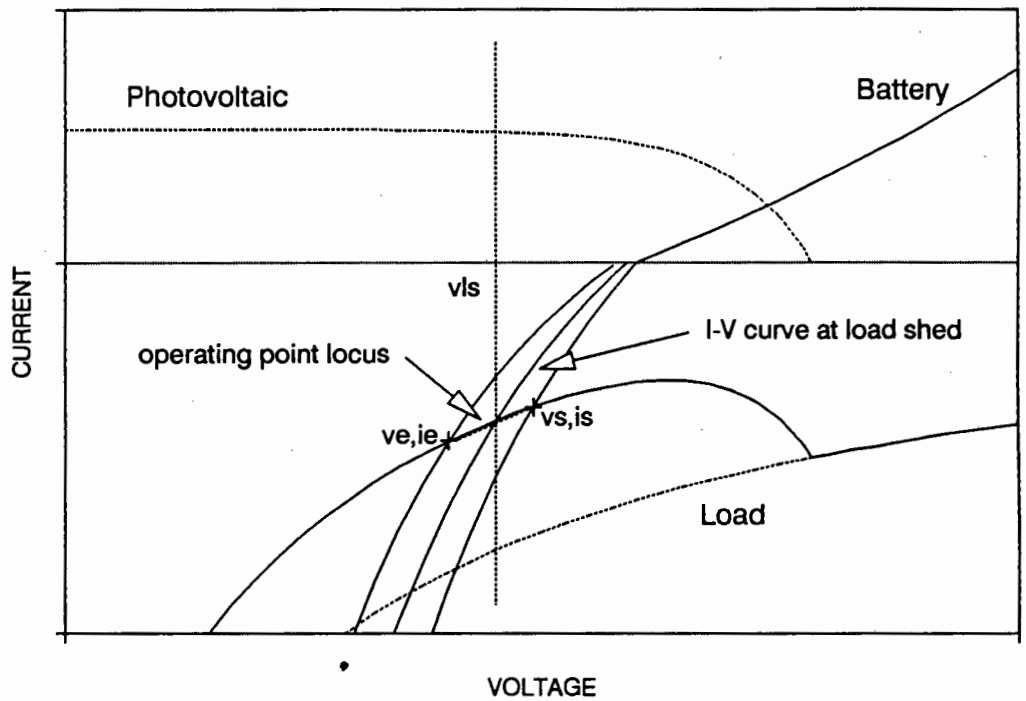

Figure 5.6 Operating points for load shed event during the hour

A simple approximation used in calculating the battery depth of discharge at the load shed point is attained by estimating the fraction of the hour at which load shed occurs. This fraction is estimated as the difference between the operating voltage at the beginning of the hour and the load shed voltage divided by the difference between the initial operating voltage and the estimated voltage at the end of the hour $((v_s - v_{ls}) / (v_s - v_e))$. Such an approximate method is justified by its simplicity and the minimal contribution that this discharge current is likely to make to the simulation as a whole.

5.5 NUMERICAL ROOT SOLVING METHOD

At the nucleus of the operating point solution procedure is a numerical root finding algorithm which determines the battery operating voltage at a point in time for a given set of I-V curves. It achieves this by finding the root of the function constituted by the regulator output I-V curve plus the load I-V curve minus the battery I-V curve. This root is the voltage level at the point of intersection of the battery I-V curve and the I-V curve which describes the nett battery current - that is, the load I-V curve (defined negative) added to the regulator output I-V curve.

This algorithm requires as input two boundary (voltage) values which bracket the root (the root of a function is bracketed by two points if the values of the function at the points have opposite signs).

To preserve modularity, the root solving algorithm is located in a separate unit. In this unit, data describing the system components (such as the battery, photovoltaic array, load, etc.), which is required for the function the root of which is to be solved, is not visible. Hence this function is located in a position in the program where such data is visible and the function itself is passed to the root solving algorithm as a function variable.

Computers use a fixed number of binary digits to represent floating point variables and, while a function may pass through zero, it is possible that its computed value is never zero for any floating point argument. It is thus necessary to decide what accuracy is appropriate for solving the root. In this case, because the root (which represents the battery operating voltage) is expected to lie in a fairly small range (close to the nominal system operating voltage), an absolute tolerance specification is suitable. In other words, convergence to the root continues until the interval between estimated roots is smaller than a specified absolute value.

The root solving method which has been implemented in PVPro is referred to here as Brent's method (refer to appendix D for details of various algorithms and the reasons for selecting this one). This method uses inverse quadratic interpolation to fit an inverse quadratic function (x as a quadratic function of y) to the function being solved at the three prior root approximations. The value of the quadratic function at the intersection of the x axis is normally taken as the next estimate of the root. However, when this estimate falls outside the bracketing bounds, or when the bounds are not collapsing rapidly enough, the algorithm takes a bisection step instead.

5.6 I-V LIMIT SPECIFICATION

As indicated above, boundary voltage limits which enclose the operating voltage must be specified for the root solving algorithm.

The lower voltage limit is specified either using the load shed voltage or the battery rest voltage. If there is no load demand, the limit is set at the battery rest voltage. Otherwise it is specified by the lower of the load shed voltage and the battery rest voltage. This is normally legitimate, but for those infrequent cases where it is necessary to ascertain the operating point while the system is in load shed state (outlined later), this limit is decreased by ten percent. Most often the new limit would bound the operating point, but if it doesn't at first, the limit is adjusted repeatedly

(decreased by ten percent each time) until it does. This approach is adopted because of the hyperbolic nature of the constant power load curve, which results in large currents at low voltage levels.

The upper voltage limit is determined either by the photovoltaic array open circuit voltage or the battery rest voltage. If there is no POA irradiance, the limit is set to the battery rest voltage, otherwise it is set to the greater of the battery rest voltage and the photovoltaic array open circuit voltage.

The current limits associated with these voltage boundary values are also calculated as these are used to determine which section of the battery I-V curves to work with. If the POA irradiance is greater than zero, the upper current limit is set by the photovoltaic array short circuit current, otherwise it is set to zero. The minimum current is set by the lower of the load currents calculated at the minimum and maximum voltage points (this would be zero for no load situations).

5.7 IMPLEMENTATION OF THE OPERATING POINT CALCULATION

The implementation of the operating point calculation process incorporates both a simple and a precise model. The simple method is based on the assumption that the battery I-V curve does not shift significantly during an hour and requires less computing time than the more precise procedure.

5.7.1. Simple Operating Point Model

The simple operating point model calculates the operating voltage at the start of the hour. This is compared with the appropriate load shed voltage (dependent on the former load shed status).

If the operating voltage is greater than the load shed voltage, the system is in the operative mode for the hour (see figure 5.7). The battery current is equal to the operating current at the start of the hour.

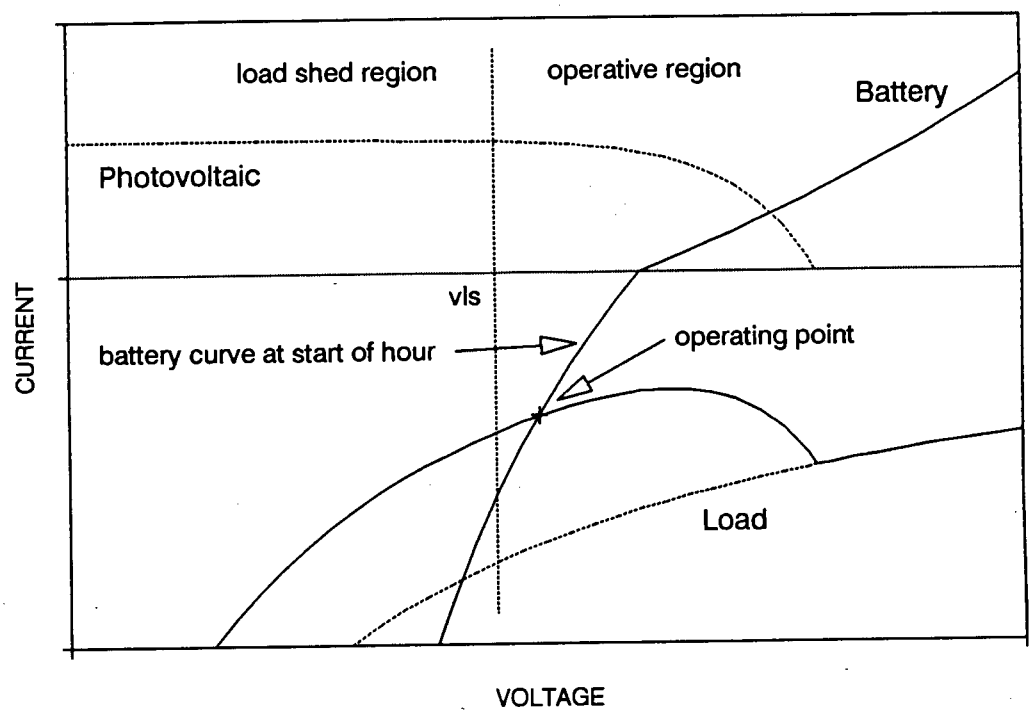

Figure 5.7 Initial operating point in operative region

On the other hand, if the operating voltage is less than the load shed voltage, the system is in load shed mode for the hour (refer to figure 5.8). If the POA irradiance is greater than zero for the hour, a new operating point is calculated at the intercept of the battery I-V curve and the photovoltaic I-V curve (modified by the regulator characteristics). This point determines the battery charging current during the load shed state.

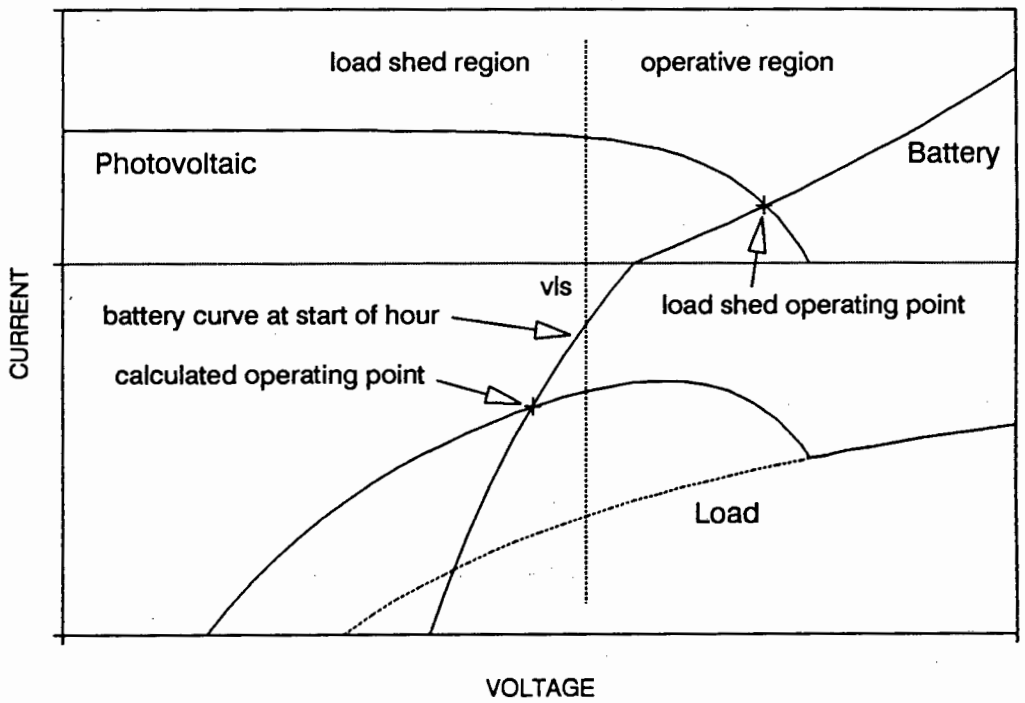

Figure 5.8 Initial operating point in load shed region

5.7.2. Complex Operating Point Model

The complex model takes into account the shift of the battery I-V curve during an hour. The operating point at the start of the hour is calculated and is compared with the appropriate load shed voltage. If this point is in the load shed region, the system is assumed to be in load shed state for the hour. Otherwise, the battery depth of discharge for the end of the hour is approximated using calculations based on the battery current at the start of the hour and the associated battery I-V curve for this depth of discharge is generated. From this, an estimated operating point for the end of the hour is calculated.

Three possible scenarios result from this procedure:

- the initial operating point is in the load shed region,
- the initial operating point is in the operative region and the final point is in the load shed region, and
- both the initial and final points are in the operative region.

In the first case, with the system in load shed mode for the hour (refer back to figure 5.8), if the POA irradiance is greater than zero for the hour, a new operating point is

calculated at the intercept between the battery I-V curve and the photovoltaic I-V curve (modified by the regulator characteristics). This point determines the battery charging current during the load shed state.

For the second eventuality, the estimated mean operating current for the hour is approximated by the average of the initial and projected final operating currents (see figure 5.9). The fraction of this current which discharges the battery before load shed is estimated as the difference between the operating voltage at the beginning of the hour and the load shed voltage divided by the difference between the initial operating voltage and the estimated voltage at the end of the hour (explained previously).

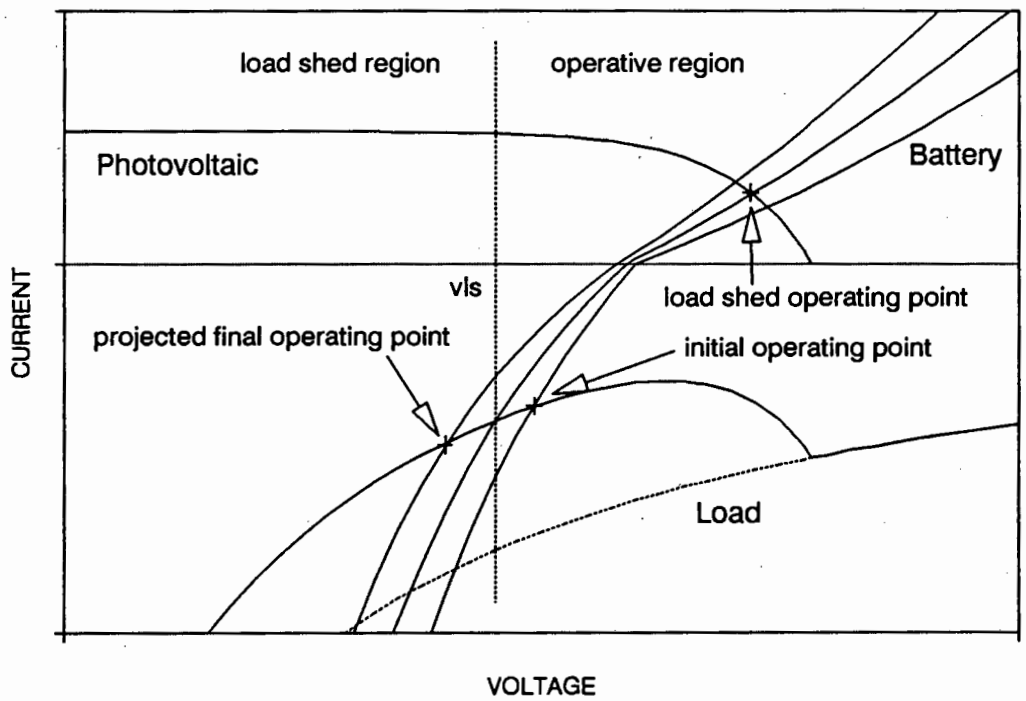

Figure 5.9 Initial operating point in operative region, final operating point in load shed region

Then, if the POA irradiance is greater than zero for the hour, the battery depth of discharge at the load shed occurrence is estimated. The new operating point (for the load shed state) is calculated at the intercept between the battery I-V curve for this depth of discharge and the photovoltaic I-V curve (modified by regulator the characteristics). The effective battery charge current is computed as the current at this point multiplied by one minus the load shed fraction calculated previously.

For the third scenario, the mean battery current for the hour is approximated by the average of the initial and projected final operating currents. Refer to figure 5.10.

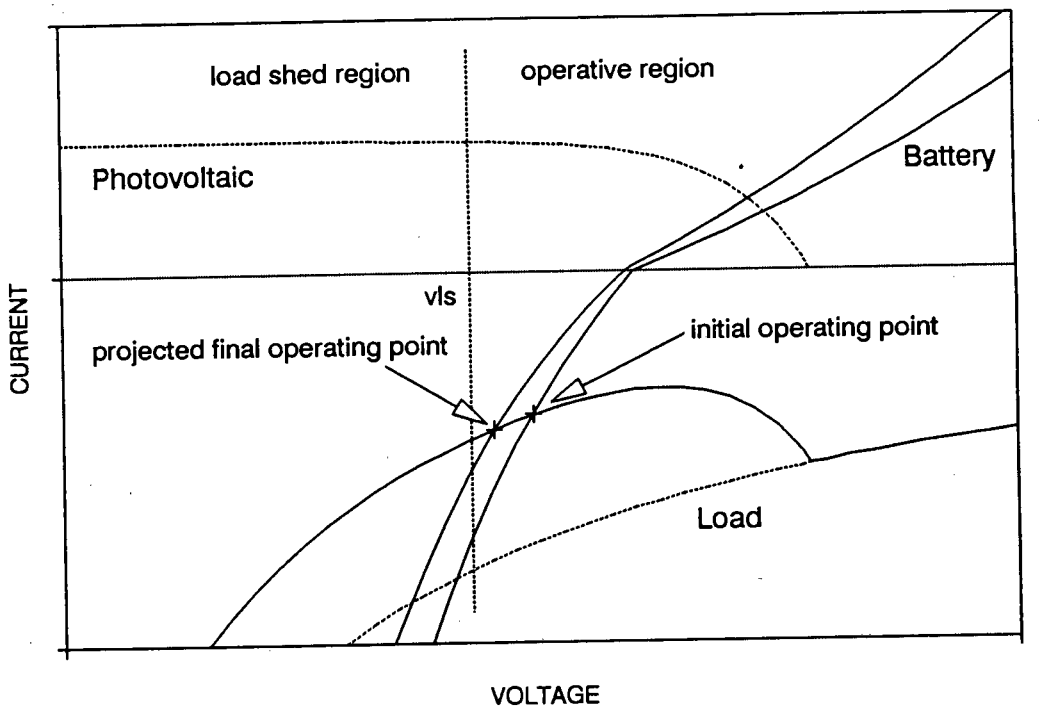

Figure 5.10 Initial and final operating points in operative region

CHAPTER 6

PROGRAM OUTPUTS

6.1 OUTPUT DURING PROGRAM EXECUTION

While the simulation procedure is executing, the current values of the following parameters are displayed on the screen: the julian day, the battery depth of discharge and the number of loss of power hours. At the end of the simulation, the predicted loss of power probability is displayed.

If the program is being executed on a system with a Hercules graphics adaptor (or true compatible), the battery depth of discharge is displayed graphically (the following graphics adaptors should also enable this, but have not been tested: CGA, MCGA, EGA, VGA, AT&T 400 line, 3270 PC and IBM-8514, and true compatibles). This feature provides a valuable overview of the system performance. For example, it shows how frequently and how deeply the batteries are being cycled, which affects the choice of battery type. It also indicates seasonal trends and whether the regulator and load shed voltage settings are satisfactory.

6.2 SUMMARISED DATA FILE

At the end of each simulation, a set of parameters which provides a summary of the system performance is written to a specified disk file. This file contains the monthly and annual totals of the following variables: the POA irradiance, the array energy, the load energy, the number of load shed hours, the battery charge energy and the battery discharge energy. In addition, the average daily maximum and minimum battery depth of discharge for each month is displayed.

The file is written in ASCII format and can therefore be viewed on the screen, edited by most word processors or dumped directly to a printer.

6.3 DETAILED DATA FILE

The program can also be configured to generate a data file on disk which logs hourly data values. The following variables can be logged: the global irradiance, the diffuse irradiance, the wind speed, the ambient temperature, the DC load power, the AC load power, the total load power, the POA irradiance, the photovoltaic cell temperature, the battery temperature, the photovoltaic array voltage, the photovoltaic array current, the regulator voltage, the regulator current, the battery voltage, the battery current, the load current, the inverter efficiency, the battery depth of discharge, the cumulative number of load shed hours and the load shed status.

This data file is potentially very large if a number of variables are selected for logging. Thus the program calculates and displays the approximate output file size whilst the user is selecting variables.

The file is also written in ASCII format and can therefore be viewed on the screen, edited by most word processors or dumped directly to a printer.

CHAPTER 7

CONCLUSIONS

A computer program has been developed successfully to simulate the performance of stand alone photovoltaic systems with battery storage on an hourly basis for one simulated year.

The program incorporates models of the POA irradiance, the photovoltaic cell temperature and the battery temperature to simulate the environmental conditions of the system. These require hourly weather data as input. Typical meteorological years, which constitute a suitable form of input weather data, have been generated for those weather stations in Southern Africa which contain sufficient data.

The energy flows within the system are simulated using models of the following parameters: photovoltaic module current, regulator efficiency and voltage, battery current and voltage, inverter efficiency, load shed voltage and load current. These models incorporate versatility in the level of modelling complexity (determined typically by the availability of the data used to characterise the components).

The various models are encapsulated in modular units to facilitate alteration and updating at a later stage.

The program is designed to simulate photovoltaic systems without maximum power point trackers, necessitating the use of interactive curve solving to compute the system operating point at any time. A robust and comprehensive algorithm has been implemented to execute this function.

In the calculation of the POA irradiance, the most recent model developed by Perez *et al.* (1987) is used. The implementation of this model in PVPro is based on the coding of the model in PVFORM, but modified to prevent computational anomalies at sunrise and sunset (consequently this correction has also been implemented in a new version of PVFORM).

Improved battery modelling has been effected using data and experience acquired from a parallel research project.

The program facilitates the economical sizing of systems in that it incorporates loss of power probability analysis and offers a high level of modelling precision. Note that judicious selection of the input weather data, with an understanding of the associated limitations, is required for this purpose.

The simulation performance of the program compared favourably with that of PVFORM (refer to appendix E). The system performance estimated by PVFORM was found to be marginally better, which is expected because PVFORM assumes that the system operates with a maximum power point tracker.

In the development of the program there has been a focus on creating an effective user interface. This is designed to simplify and speed up program operation, and to present output in a form which is useful and illustrative. The finished product constitutes a meaningful step forward in improved computer simulation of photovoltaic systems.

CHAPTER 8

RECOMMENDATIONS

Empirical data from monitored photovoltaic systems should be used to verify the simulation program. The program should then be used to assess other simulation and sizing techniques.

The program should be extended to simulate hybrid remote area power supply systems. The modelling of wind, diesel, petrol and hydro powered generators should be considered.

The development of a technique which uses the simulation structure for automatic system sizing should be considered. This might involve the collaborative use of a simple analytical sizing technique, or optimisation through the analysis of the sensitivity of the system to variation of the fundamental parameters.

An economic package should be considered in the further development of PVPro for the assessment of the long-term economic potential of photovoltaic systems. This would enable photovoltaic systems to be compared on an economic basis with other competing systems or with differently configured photovoltaic systems.

LIST OF REFERENCES

Burden, R. L. and J.D. Faires (1985). *Numerical Analysis*. Prindle, Weber and Schmidt, Boston.

Edenburg, M.W. (1981). Analytical Models for Solar Photovoltaic Energy System Components. Sandia National Laboratories, Albuquerque.

Evans, D.L, W.A. Facinelli and R.T. Otterbein (1978). Combined Photovoltaic/Thermal Systems Studies. Sandia National Laboratories, Albuquerque.

Fuentes, M.K. (1987). A simplified thermal model for flat-plate photovoltaic arrays. SAND85-0330 (revised), Sandia National Laboratories, Albuquerque.

Gonzalez, C., G. Hill and R. Ross (1982). Characterization of the Electrical Output of Flat-Plate Photovoltaic Arrays. *Proceedings*. 16th Annual IEEE Photovoltaic Specialists Conference.

Hay, J.E. and D. McKay (1985). Estimating solar irradiance on inclined surfaces: a review and assessment of methodologies. *International Journal of Solar Energy*, 3, 203-240.

Hoover, E.R. (1980). Solcel-II: An Improved Photovoltaic System Computer Program. *Proceedings*, 14th Annual IEEE Photovoltaic Specialists Conference, 1258-1261.

Lambarski, T.J., A.F. Malmberg, K.E. Melick, R.M. Turfler and M.G. Semmens (1978). Photovoltaic Transient Analysis Program User's Guide, Vol. 2: Guide to Photovoltaic Elements. Sandia National Laboratories, Albuquerque.

Liu, B.Y.H. and R. Jordan (1963). The long term average performance of flat-plate solar-energy collectors. *Solar Energy*, 7, 53-74.

Menicucci, D.F. and J.P. Fernandez (1988). User's manual for PVFORM: a photovoltaic system simulation program for stand-alone and grid-interactive applications. SAND85-0376 (revised), Sandia National Laboratories, Albuquerque.

Perez, R., R. Seals, P. Ineichen, R. Stewart and D. Menicucci (1987). A new simplified version of the Perez diffuse irradiance model for tilted surfaces. *Solar Energy*, 39, 221-231.

Pissimanis, D., G. Karras, V. Notaridou and K. Gavra (1988). The generation of a "typical meteorological year" for the city of Athens. *Solar Energy*, 40, 405-411.

Press, W.H., B.P. Flannery, S.A. Teukolsky and W.T. Vetterling (1986). *Numerical Recipes: The Art of Scientific Computing*. Cambridge University Press, New York.

Purcell, C.P. (1990). *Battery Performance in Stand Alone Photovoltaic Systems.* Unpublished Masters dissertation. Energy Research Institute, University of Cape Town.

Rauschenbach, H.S. (1980). *Solar cell array design handbook.* Van Nostrand Reinhold Company, New York.

APPENDIX A

EVALUATION OF TWO EXISTING PHOTOVOLTAIC SYSTEM PERFORMANCE PROGRAMS

Two state-of-the-art photovoltaic system performance programs based on computations on an hourly basis, one from Sandia National Laboratories (PVFORM) and one developed at the Asian Institute of Technology, are evaluated in this appendix to assess their respective merits and deficiencies.

ASIAN INSTITUTE OF TECHNOLOGY PROGRAM

The program developed at the Asian Institute of Technology is designed specifically as a sizing tool. In each sizing process, it evaluates the performance of a number of systems comprising different photovoltaic array and battery sizes, and hence utilises simplified component models to improve execution speed.

The input hourly global solar irradiance data is generated by a binomial distribution irradiance model which does not take into consideration seasonal variations or correlation between successive hourly irradiance values.

The daily ambient temperature profile is approximated by a sinusoidal distribution, with daily maximum and minimum ambient temperatures and overall seasonal variation of these parameters being specified.

The array temperature model is based on empirical formulae with simplified theoretical considerations.

The model used for the photovoltaic array I-V curve is based on the one detailed by Rauschenbach (1980) described in the appendix on photovoltaic I-V curve models. This model is used to generate a reference I-V curve at a specified irradiance and temperature, and other curves for different irradiance and temperature levels are obtained by translation from this reference curve.

The system load profile is described by one of three different daily load profiles: a constant load, a constant load with a peak for a single hour and a cosine-shaped load. Only DC loads are considered, obviating the need for an inverter model.

The regulator is modelled simply as a switch which disconnects the battery from the photovoltaic array when it is fully charged. Similarly, the load is disconnected from the battery when the battery charge drops below a specified value.

The battery model is a simple internal charge / discharge resistance model. Charge accounting is done on a watt-hour basis.

The system operating voltage is assumed to be 12 volts.

Most of these models and techniques are simplistic and are thus unsuitable for precision simulation. In addition, the program is coded in Basic, a slow language which is unsuitable for large or complex program structures. The only features from the program which are suitable for enhancement are the photovoltaic and battery models.

SANDIA NATIONAL LABORATORIES PROGRAM

A precision hourly simulation program, PVFORM, has been developed at Sandia National Laboratories.

The program requires an entire set of hourly weather data for a year as input, providing the user with the option of how to generate or capture this input data.

The load profile can be specified either as a single daily profile which is repeated throughout the year, or as a set of hourly load values for the entire year.

The anisotropic model developed by Perez *et al* (1987) is used to estimate the diffuse irradiance on the plane of array. This model is widely-accepted and well-established. Certain assumptions used in the implementation of the model in PVFORM are erroneous at sunrise and sunset and occasionally result in anomalous values.

The photovoltaic cell temperature is calculated by a model developed by Fuentes (1987). This thermal model requires a minimum of input and has been found experimentally to have an error of less than 5°C. The model, being iterative, calculates an initial approximation of the cell temperature and then uses this estimation to formulate a closer approximation. In the implementation in PVFORM, this process is repeated ten times to ensure adequate convergence of the result.

The photovoltaic module power output is calculated using the array efficiency. The efficiency is computed by modifying a specified reference efficiency with a temperature dependent coefficient.

Two curves, one of charge efficiency and the other of discharge efficiency (as a function of the state of charge), constitute the battery model. This model simulates the battery only in terms of energy flows.

The inverter model is one which has been determined by fitting a third order polynomial through a set of empirical efficiency measurements (from ten to one hundred percent of full load) for a number of typical inverters. For loads less than ten percent of full load a linear efficiency curve is assumed.

The program is coded in FORTRAN, a language which is fast for mathematical functions but does not facilitate the development of a powerful user-interface.

This program is based primarily on models simulating energy flows within the photovoltaic system. Such an energy-oriented approach is suitable for a system with a maximum power point tracker, since the operating voltages are determined by such a device. However, for systems without maximum power point trackers, the operating currents and voltages within the systems need to be calculated interactively and suitable voltage and current models are required.

The photovoltaic cell temperature model and the anisotropic diffuse irradiance model (with appropriate modification to prevent calculation errors at sunrise and sunset) are suitable for precision simulation.

APPENDIX B

TYPICAL METEOROLOGICAL YEAR GENERATION METHODOLOGY

INTRODUCTION

The requirement for weather data suitable for computer-based energy modelling programs has resulted in the establishment of a methodology for the generation of a category of data sets known as typical meteorological years. These comprise a full set of 8760 hourly weather observations containing real weather sequences that is intended to represent the long-term climatic mean conditions for a particular location.

METEOROLOGICAL DATABASE

Meteorological data sets consisting of ambient temperature, wind speed, and global and diffuse irradiance were available from the South African Weather Bureau for the follow primary stations: Alexander Bay, Bloemfontein, Cape Town, Durban, Grootfontein (Cape), Keetmanshoop, Nelspruit, Port Elizabeth, Pretoria (average of the data from Forum, Irene and Lynnwood Road), Roodeplaat, Upington and Windhoek.

The data sets contained as much data as was available on magnetic tape from the weather bureau (extending as far back as 1950 in many cases). A significant portion of ambient temperature data was unavailable and there was no wind data for Roodeplaat and Nelspruit.

METHODOLOGY

For every location, a typical meteorological month (TMM) for each of the twelve calendar months was selected from the long term data base. This process consisted of two stages.

In the first, candidate months of five different years for each calender month were selected. The following meteorological parameters, referred to as indices, were used in the selection process:

- the daily maximum value, minimum value, mean and range of the wind speed and ambient temperature, and
- the total daily global and direct irradiance (the direct irradiance being calculated from the total daily global and diffuse irradiance).

The cumulative distribution function (CDF) of each index was calculated for each calendar month for individual years and for the full data set. The CDF gives the proportion of values which are less than or equal to a specified value of an index. The CDF for the variable x was approximated by $S_n(x)$:

$$S_n(x) = \begin{cases} 0 & \text{for } x < x_1 \\ (k - 0.5) / n & \text{for } x_k < x < x_{k+1} \\ 1 & \text{for } x > x_n \end{cases}$$

where:

x_k is the k^{th} ordered (from smallest to largest) observation and n is the number of observations on the variable x.

The CDFs of the individual years were compared with the CDF of the full data set using the Finkelstein-Schafer statistic (FS):

$$FS = \left(\sum_{i=1}^{n} \Delta_i\right) / n$$

where:

Δ_i is the absolute difference between the long term CDF and the individual CDF at x_i (i = 1, 2 ... n), and

n is the number of readings in the month under consideration.

The closer the long term CDF is to the individual CDF, the smaller the value of FS. For each individual year ten FS statistics were computed: one for each of the ten indices.

The ten FS values were combined into one statistic, the weighted sum (WS) according to the following formula:

$$WS = \sum_{i=1}^{10} w_i \times FS_i$$

where:

w_i is the weighting associated with each index, and

FS_i is the FS value for each index.

The w_i values used were as follows:

Wind	maximum	0.0889
	minimum	0.0222
	range	0.0111
	average	0.0445
Ambient Temperature	maximum	0.1754
	minimum	0.0175
	range	0.0351
	average	0.1053
Global Irradiance	daily total	0.2500
Direct Irradiance	daily total	0.2500

The WS value of each individual year was calculated and the five years with the smallest WS values were selected as candidate years for the month in question.

In the second stage of the selection process, a single typical meteorological month was selected from the five candidate years. The parameters used in this selection procedure were the average total daily global and diffuse irradiance of each month of each individual year as well as for each month over the whole data set, and the number of missing data values in each month.

FINAL PRODUCT

Typical meteorological years were generated for the following stations:

Station	Grade
Cape Town	A
Durban	A
Port Elizabeth	A
Alexander Bay	B
Keetmanshoop	B
Bloemfontein	C
Pretoria	C
Upington	C
Windhoek	C

The TMYs were graded according to the amount of data available (indicated by the approximate number of years of data) for the selection of the TMMs:

Grade	Data Size
A	20
B	15
C	12

Due to lack of data, TMYs were not generated for Grootfontein, Roodeplaat and Nelspruit.

APPENDIX C

COMPARISON OF PHOTOVOLTAIC I-V CURVE MODELS

This appendix presents a summarised evaluation of suitable photovoltaic I-V curve models located via a literature search. The models are based on fundamental photovoltaic characteristics such as short circuit current, open circuit voltage, shunt resistance etc. They are required to generate curves at any POA irradiance level and cell temperature within the normal operating range (for systems without concentrators), derived from a base I-V curve at a reference POA irradiance level and cell temperature.

Photovoltaic I-V curve data was obtained for the most popular panels from major suppliers in South Africa: the BP 245 and 340 and the Arco M55, M65, M75, G4000 and G100. The data is in the format of two sets of I-V curves: one for a fixed cell temperature (eg 25°C) and a range of POA irradiance (eg 1000, 800, 600, 400 and 200 Wm^{-2}), and the other for a fixed irradiance (eg 1000 Wm^{-2}) and a range of cell temperatures (eg 25, 40, 60 and 80°C). The effects of irradiance and cell temperature on the curves are assumed independent, and the following parameters can be determined from each of the curves: I_{sc}, V_{oc}, I_{mp} and V_{mp}.

The basic tool for the comparison of the models was an I-V curve generation program. The voltage and current axes of the generated curves were scalable so that the printed output of the program could be directly superimposed on the original I-V curves.

Each of the models described here is identified by a reference to the text that describes it. Following this is a list of the basic inputs it requires and a brief outline of the simulation methodology, if appropriate. Finally there is a discussion of the merits and disadvantages of the model.

The variables being solved in the equations listed in the simulation methodology are highlighted in bold.

Phang, JH., D.S.H. Chan and J.R. Philips (1984). Accurate analytical method for the extraction of solar cell model parameters. *Electronics Letters*, 20, 406-408.

Base Inputs

V_{oc} I_{sc} V_{mp} I_{mp} R_{so} R_{sho} T_{pv}

Method

$$R_{sh} = R_{sho}$$

$$V_t = k \times T_{pv} / q \; (= T_{pv} / 11609)$$

$$n = (V_{mp} + I_{mp} \times R_{so} - V_{oc}) / (V_t \times (\text{Ln}\,(I_{sc} - V_{mp} / R_{sho} - I_{mp}) - \text{Ln}\,(I_{sc} - V_{oc} / R_{sh}) + I_{mp} / (I_{sc} - V_{oc} / R_{sho}))$$

$$I_s = (I_{sc} - V_{oc} / R_{sh}) \times \text{Exp}\,(-V_{oc} / (n \times V_t))$$

$$R_s = R_{so} - n \times V_t / I_s \times \text{Exp}\,(-V_{oc} / (n \times V_t))$$

$$I_{ph} = I_{sc} \times (1 + R_s / R_{sh}) + I_s \times (\text{Exp}\,(I_{sc} \times R_s / (n \times V_t)) - 1)$$

$$I_{pv} = I_{ph} - (V_{pv} + I_{pv} \times R_s) / R_{sh} - I_s \times (\text{Exp}\,((V_{pv} + I_{pv} \times R_s) / (n \times V_t)) - 1))$$

Discussion

This model is based on a single diode lumped parameter equivalent circuit of a solar cell model and provided a good fit over the range of curves it was tested on (worst case error approximately fifteen percent and average error about two percent for the base curves).

A disadvantage of such a model, requiring shunt and series resistances as inputs, is that these parameters are usually determined graphically from inadequately defined I-V curves ($R_{so} = -\delta V_{pv} / \delta I_{pv}$ at $V_{pv} = V_{oc}$ and $R_{sho} = -\delta V_{pv} / \delta I_{pv}$ at $I_{pv} = I_{sc}$). Also, this is a cell model and the usage of array parameters usually results in computational errors (the exponential calculations become too large). Thus array parameters have to be scaled to acceptable cell parameter values.

The model does not cater for a range of POA irradiance and cell temperature levels. A possible method of extending the basic model to simulate I-V curves at various irradiance and temperature levels is to fit curves to each of the input parameters over the range of irradiance and temperature of interest. Hence, there would be functions which describe the variation of V_{oc}, I_{sc}, V_{mp}, I_{mp}, R_{so} and R_{sho} with temperature and

irradiance. To generate a curve at a given irradiance and temperature level, the input parameters derived from these functions would be used as input to the basic model. Of these, the current and voltage parameters indicate fairly linear trends and could be approximated adequately by straight line curves. However, the resistance parameters do not display significant trends and would be effectively approximated only by a high order polynomial fit. Usage of such parameters, which do not display significant trends, in determining the shape of the I-V curve is neither intuitive nor elegant.

Charles, J.P., M. Abdelkrim, Y.H. Muoy and P. Mialhe (1981). A practical method of analysis for the current-voltage characteristics of solar cells. *Solar Cells*, 4, 169-178.

Discussion

This model is based on the identical single diode lumped parameter equivalent circuit of a solar cell as the previous one. However, the methodology for determining the parameters is more complex, including the solving of nonlinear simultaneous equations which requires extensive computation and good initial estimates for convergence. It is consequently of no further interest here.

Chan, D.S.H. and JH. Phang (1987). Analytical methods for the extraction of solar-cell single- and double-diode model parameters from I-V characteristics. *IEEE Transactions on Electron Devices*, ED-34, 286-293.

Base Inputs

V_{oc} I_{sc} V_{mp} I_{mp} R_{so} R_{sho} T_{pv}

Method

$V_t = k \times T_{pv} / q \; (= T_{pv} / 11609)$

$\alpha = I_{sc} - V_{oc} / R_{sho}$

$\beta = I_{sc} - I_{mp} - V_{mp} / R_{sho}$

$\gamma = \text{Exp}\,((V_{mp} - V_{oc}) / (2 \times V_t))$

$\delta = I_{mp} / V_t$

$a = \alpha \times \gamma \times \delta \times (1 - \gamma)$

$$b = \alpha \times \gamma \times (2 - \gamma) + \alpha \times \gamma \times \delta \times R_{sho} \times (\gamma - 1) - \beta + \gamma \times \delta \times V_t \times (1 - 2 \times \gamma)$$

$$c = \alpha \times \gamma \times R_{so} \times (\gamma - 2) + \beta \times R_{so} + 2 \times \gamma \times V_t \times (1 - \gamma)$$

$$R_s = (-b + \sqrt{(b \times b - 4 \times a \times c)}) / (2 \times a)$$

$$I_{s1} = (V_{oc} / R_{sho} - I_{sc} + 2 \times V_t / (R_{so} - R_s)) \times \text{Exp}(-V_{oc} / V_t)$$

$$I_{s2} = 2 \times (I_{sc} - V_{oc} / R_{sho} - V_t / (R_{sho} - R_s)) \times \text{Exp}(-V_{oc} / (2 \times V_t))$$

$$R_{sh} = 1 / (1 / (R_{sho} - R_s) - I_{s1} / V_t \times \text{Exp}(I_{sc} \times R_s / V_t) - I_{s2} / (2 \times V_t) \times \text{Exp}(I_{sc} \times R_s / (2 \times V_t)))$$

$$I_{ph} = I_{s1} \times (\text{Exp}(V_{oc} / V_t) - 1) + I_{s2} \times (\text{Exp}(V_{oc} / (2 \times V_t)) - 1) + V_{oc} / R_{sh}$$

$$I_{pv} = I_{ph} - (V_{pv} + I_{pv} \times R_s) / R_{sh} - I_{s1} \times (\text{Exp}((V_{pv} + I_{pv} \times R_s) / V_t) - 1) - I_{s2} \times (\text{Exp}((V_{pv} + I_{pv} \times R_s) / (2 \times V_t)) - 1)$$

Discussion

The article provides useful background on single and double diode lumped circuit models, and provides practical methods of implementing them (the single diode model is outlined above in the description of the article by Phang *et al.* (1984)). The double diode model, detailed here, is alleged to be more accurate than the single diode model and potential problems of the latter are outlined in the paper (for example, low illuminations resulting in negative series resistance values).

In practice the double diode model was found to generate I-V curves with a similar precision to the single diode model: in some cases the fit was slightly better, in other cases slightly worse.

The overall analysis of the single diode model applies to this model as well, although this model is slightly more complex in its implementation.

Goldstein, L.H. and G.R. Case (1978). PVSS - A photovoltaic system simulation program. *Solar Energy*, 21, 37-43.

Discussion

The inputs required by the model described in this article are not easily derived from the I-V curve data available. For example, a device specific constant is used, yet no method is outlined for the derivation of this constant. Hence the model was not considered further.

Singer, S., B. Rozenshtein and S. Surazi (1984). Characterization of PV array output using a small number of measured parameters. *Solar Energy*, 32, 603-607.

Base Inputs

V_{oco} I_{sco} P_{mpo} Q_{pvo} T_{pvo} Q_{pv} T_{pv} $\Delta V_{oc}\Delta Q_{pv}$ $\Delta I_{sc}\Delta Q_{pv}$ $\Delta P_{mp}\Delta Q_{pv}$ $\Delta V_{oc}\Delta T_{pv}$ $\Delta I_{sc}\Delta T_{pv}$ $\Delta P_{mp}\Delta T_{pv}$

Method

$$\mathbf{I_{sc}} = I_{sco} \times \Delta I_{sc}\Delta Q_{pv} \times (Q_{pv} - Q_{pvo}) + \Delta I_{sc}\Delta T_{pv} \times (T_{pv} - T_{pvo})$$

$$\mathbf{V_{oc}} = V_{oco} \times \Delta V_{oc}\Delta Q_{pv} \times (Q_{pv} - Q_{pvo}) + \Delta V_{oc}\Delta T_{pv} \times (T_{pv} - T_{pvo})$$

$$\mathbf{P_{mp}} = P_{mpo} \times \Delta P_{mp}\Delta Q_{pv} \times (Q_{pv} - Q_{pvo}) + \Delta P_{mp}\Delta T_{pv} \times (T_{pv} - T_{pvo})$$

$$0 = \mathbf{I_{mp}} \times (1 + 1 / 20.7 \times (\mathbf{I_{mp}} / (I_{sc} - \mathbf{I_{mp}}) + \mathrm{Ln}((I_{sc} - \mathbf{I_{mp}}) / I_{sc}))) - 2 \times P_{mp} / V_{oc}$$

$$\mathbf{R} = P_{mp} / I_{mp} / I_{mp} - V_{oc} / 20.7 \times (1 / (I_{sc} - I_{mp}))$$

$$\mathbf{I_{pv}} = I_{sc} \times (1 - 1 \times 10^{-9} \times \mathrm{Exp}(20.7 / V_{oc} \times (V_{pv} + \mathbf{I_{pv}} \times R)))$$

Discussion

This model is based on an adapted (and simplified) form of the basic solar cell equation derived from solid-state physics theory.

The authors claim an accuracy of three percent for the original base curve and about six percent for other curves derived from this one at various irradiance intensities and cell temperatures. These assertions appeared somewhat optimistic, with worst case errors for the generated base curves of up to about twelve percent. For curves derived from the base curve for other irradiance and temperature levels, the errors were up to sixteen percent (average approximately three percent).

The method described here is a slightly modified form of the original which was found to generate more accurate curves over a range of irradiance and cell temperature levels. In this modification, the variation of the voltage, current and power parameters are assumed to be linear over the relevant radiance and temperature range.

Rauschenbach, H.S. (1980). *Solar cell array design handbook.* Van Nostrand Reinhold Company, New York.

Base Inputs

V_{oco} I_{sco} I_{mpo} V_{mpo} Q_{pvo} T_{pvo} Q_{pv} T_{pv} $\Delta V_{oc}\Delta Q_{pv}$ $\Delta I_{sc}\Delta Q_{pv}$ $\Delta V_{mp}\Delta Q_{pv}$ $\Delta I_{mp}\Delta Q_{pv}$ $\Delta V_{oc}\Delta T_{pv}$ $\Delta I_{sc}\Delta T_{pv}$ $\Delta V_{mp}\Delta T_{pv}$ $\Delta I_{mp}\Delta T_{pv}$

Method

$$
\begin{aligned}
I_{sc} &= I_{sco} + \Delta I_{sc}\Delta Q_{pv} \times (Q_{pv} - Q_{pvo}) + \Delta I_{sc}\Delta T_{pv} \times (T_{pv} - T_{pvo}) \\
V_{oc} &= V_{oco} + \Delta V_{oc}\Delta Q_{pv} \times (Q_{pv} - Q_{pvo}) + \Delta V_{oc}\Delta T_{pv} \times (T_{pv} - T_{pvo}) \\
I_{mp} &= I_{mpo} + \Delta I_{mp}\Delta Q_{pv} \times (Q_{pv} - Q_{pvo}) + \Delta I_{mp}\Delta T_{pv} \times (T_{pv} - T_{pvo}) \\
V_{mp} &= V_{mpo} + \Delta V_{mp}\Delta Q_{pv} \times (Q_{pv} - Q_{pvo}) + \Delta V_{mp}\Delta T_{pv} \times (T_{pv} - T_{pvo}) \\
C_2 &= (V_{mp} / V_{oc} - 1) / \mathrm{Ln}\,(1 - I_{mp} / I_{sc}) \\
C_1 &= (1 - I_{mp} / I_{sc}) \times \mathrm{Exp}\,(-V_{mp} / (C_2 \times V_{oc})) \\
I_{pv} &= I_{sc} \times (1 - C_1 \times (\mathrm{Exp}\,(V_{pv} / (C_2 \times V_{oc})) - 1))
\end{aligned}
$$

Discussion

Three different analytical models are described in this text. The first requires input which is not easily derived from the I-V curve data available. The second involves the complex numerical solving of an equation which yields multiple roots, of which one is to be selected. The complexity of this process precludes the model from simple computer implementation.

A slightly modified (and improved) version of the third model is described in more detail here. This model is also based on an adapted (and simplified) form of the basic solar cell equation derived from solid-state physics theory.

Worst case errors for the generated base curves were up to about thirteen percent. For the curves derived from the base curve for other irradiance and temperature levels, the errors were up to about seventeen percent (average approximately three percent). A more detailed analysis of the performance of this model is described in the main body of this text.

The basic model described in the text has been extended to cater for the generation of curves at a variety of POA irradiance and cell temperature levels. The variation of the

voltage and current parameters are assumed to be linear over the relevant radiance and temperature range.

This model is exceptionally simple in its implementation (it is the only one described here which does not rely on numerical methods for solution). It facilitates simple extrapolation of the base curve for a variety of irradiance and temperature levels, and offers the same precision as the best of the other models. Hence this model was selected for implementation in the simulation program.

APPENDIX D

SELECTION OF ROOT SOLVING ALGORITHM

The selection of an appropriate root solving algorithm is dependent on the nature of function under consideration. The algorithm used in PVPro determines the battery operating voltage for a given set of I-V curves by finding the root of the function constituted by the regulator output I-V curve plus the load I-V curve minus the battery I-V curve. This function is constituted by a number of diverse formulae and is not in any particularly convenient format.

There are a number of established methods for solving roots numerically (refer to Burden and Faires, 1985, and Press *et al.*, 1986, for comprehensive details). Of these, methods which operate only on polynomials, such as the Newton-Horner and Laguerre method, are unsuitable. Those which require the first derivative of the function, such as the Newton-Raphson method, and those designed for complex functions, such as Muller's method, are also inappropriate. This leaves the following standard methods for consideration: the bisection, secant, false position and Brent methods.

The bisection method evaluates the function at the midpoint of the bracketed interval and examines it sign. This midpoint then replaces the boundary at which the function has the same sign, and the process is repeated until the interval decreases to less than the specified tolerance.

For functions that are smooth near the root, the secant method generally converges faster than bisection. In this method, the new approximation of the root is taken as the point where a straight line between the points on the function at the previous two root approximations intersects the x-axis. After each iteration, the two most recent of the prior estimates are retained and the process is repeated. This method has the disadvantage that the root does not necessarily remain bracketed and can thus not be guaranteed to converge for functions which are not sufficiently continuous.

This disadvantage is overcome in the false position method, which uses the same procedure as the secant method to obtain a new approximation for the root. However, the prior estimate for which the function value has opposite sign from the function value at the current best estimate of the root is retained, so that the two root estimates continue to bracket the root. This method does not converge in general as fast as the secant method.

While the secant and false position methods can be shown formally to converge faster than the bisection method, there are in practice a number of functions for which bisection converges more rapidly. Bisection always halves the interval, while secant and false position can sometimes spend many cycles pulling distant bounds closer to a root.

A method has been devised which combines the advantages of both types of methods. While the secant and false position methods assume approximately linear behaviour between two prior root estimates, this method, referred to here as Brent's method, uses inverse quadratic interpolation to fit an inverse quadratic function (x as a quadratic function of y) to three prior points. The value of the quadratic function at $y = 0$ is normally taken as the next estimate of the root. However, when this estimate falls outside the bounds or when the bounds are not collapsing rapidly enough, the algorithm takes a bisection step instead to guarantee an adequate rate of convergence.

Brent's method has been implemented in PVPro because it effects more rapid convergence for a broader range of functions than the other methods, without being considerably more complex and with a guarantee of convergence.

APPENDIX E

COMPARISON OF PVFORM AND PVPRO SIMULATION PERFORMANCE

An appropriate system configuration was established to compare the simulation performance of PVFORM with that of PVPro. This configuration was selected such that it could be characterised easily for both programs and that the performance of the programs would be tested thoroughly. The graphical output of the simulated system performance, estimated by PVPro, is shown in figure E1.

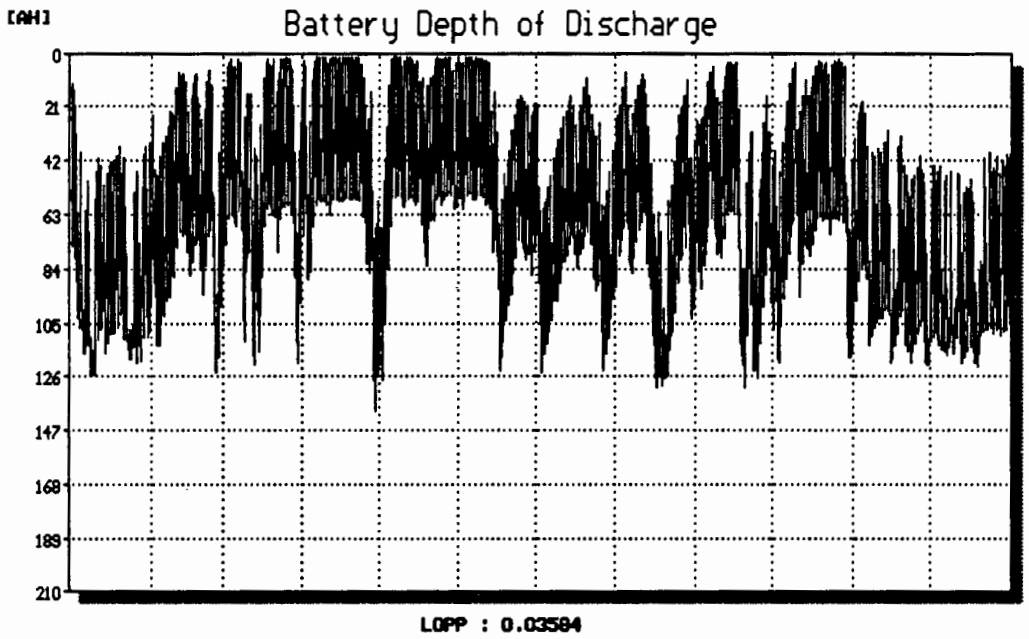

Figure E1 Graphical output of the system performance simulated by PVPro

Simulated monthly and annual performance statistics were compared. The plane of array irradiance estimation was practically identical for both programs. The monthly photovoltaic array energy outputs predicted by PVFORM were between three and seven percent greater than the corresponding estimations of PVPro, and over the entire year PVFORM's prediction was four percent more than that of PVPro. The difference could be attributed to the fact that PVFORM assumes that the system operates with a maximum power point tracker, whereas PVPro does not.

The predicted average daily minimum battery state of charge over the year was almost identical for both programs. On a monthly basis, the difference between the estimation of this parameter by the two programs was between zero and ten percent

of the estimation by PVPro. PVFORM predicted an average daily maximum battery state of charge over the year which was three percent more than the value estimated by PVPro. On a monthly basis, the difference in the estimation of this parameter by the two programs varied by between two and six percent of the PVPro estimation, with PVFORM predicting a higher value for eleven months of the year (this may be related to the increased simulated array output of PVFORM).

The difference in the estimation by the two programs of the energy supplied to the load was negligible for those months with no loss of power hours. PVFORM assumes that the load demand is met by a backup device when the photovoltaic supply system is in load shed state, and therefore its estimation of the energy supplied to the load is independent of a load shed occurrence. PVPro does incorporate load shed occurrences in its estimation. This difference was reflected in the programs' estimations of the energy supplied to the load, with PVPro's estimation being less than that of PVFORM for months with load shed occurrences (the greater the number of load shed occurrences, the greater was the difference between the estimations).

The estimated loss of power probability of the system was 0.036 for PVPro and 0.032 for PVFORM. The monthly profiles of the loss of load hours were similar for both programs. The slightly higher loss of power probability of PVPro may be partly attributed to the higher array energy output predicted by PVFORM.

From these results, it can be seen that both programs estimate similar system performances. As expected, the system performance predicted by PVFORM (with a maximum power point tracker) is slightly better than that of PVPro (without a maximum power point tracker).